Table 3. *Timetable of the stages in each cycle of WLL*

| Case | Left/Right | No. of Cycles | Total Time, s | Mean Time ± SD, s* | | | | |
|---|---|---|---|---|---|---|---|---|
| | | | | Each Cycle, s† | Stage a, Instilling, s | Stage b, Retaining, s | Stage c, Draining, s | Stage d, Preparing, s |
| 1 | L | 20 | 6260 | 258 ± 15.0 | 42 ± 3.0 | 120 ± 1.6 | 83 ± 42.2 | 13 ± 18.6 |
| | R‡ | 11 | 6895 | 561 ± 161.7 | 41 ± 8.1 | 425 ± 196.2 | 59 ± 16.4 | 8 ± 2.6 |
| 2 | L | 20 | 5200 | 210 ± 21.9 | 28 ± 3.0 | 120 ± 0 | 52 ± 23.2 | 13 ± 5.1 |
| | R | 20 | 5450 | 220 ± 8.3 | 45 ± 5.9 | 120 ± 0 | 52 ± 16.1 | 8 ± 8.1 |
| 3 | L | 20 | 5583 | 237 ± 15.1 | 36 ± 7.0 | 120 ± 0 | 73 ± 18.4 | 10 ± 2.6 |
| | R | 20 | 6060 | 236 ± 38.8 | 35 ± 6.0 | 120 ± 0 | 64 ± 26.8 | 20 ± 16.8 |
| 4 | L | 24 | 5926 | 215 ± 19.4 | 35 ± 4.1 | 120 ± 0 | 54 ± 24.7 | 10 ± 3.3 |
| | R | 29 | 9018 | 285 ± 17.5 | 57 ± 3.9 | 120 ± 0 | 102 ± 16.8 | 8 ± 3.3 |
| 5 | L | 20 | 5230 | 227 ± 30.6 | 31 ± 11.9 | 120 ± 0 | 76 ± 31.9 | 11 ± 4.7 |
| | R | 20 | 6480 | 284 ± 25.3 | 31 ± 6.2 | 120 ± 0 | 121 ± 20.2 | 19 ± 24.8 |
| 6 | L | 20 | 5395 | 266 ± 32.3 | 10 ± 0 | 120 ± 0 | 133 ± 32.0 | 5 ± 0 |
| | R | 20 | 5680 | 278 ± 42.2 | 28 ± 11.2 | 132 ± 24.6 | 112 ± 24.8 | 5 ± 0 |
| 7 | R | 20 | 6180 | 283 ± 31.6 | 52 ± 10.1 | 120 ± 0 | 109 ± 41.4 | 13 ± 11.5 |
| 8 | L | 16 | 10380 | 634 ± 264.9 | 180 ± 32.1 | 199 ± 28.7 | 148 ± 50.0 | 96 ± 250.3 |
| | R | 20 | 11796 | 550 ± 49.5 | 188 ± 41.3 | 200 ± 6.2 | 153 ± 20.5 | 16 ± 20.6 |
| 9 | L | 11 | 6180 | 553 ± 185.8 | 146 ± 42.8 | 193 ± 24.2 | 174 ± 82.2 | 40 ± 112.3 |
| | R | 13 | 8280 | 627 ± 98.1 | 225 ± 45.2 | 231 ± 64.1 | 225 ± 63.3 | 0 ± 0 |

*Data are presented as a mean ± SD of time (s) required for 1 lavage cycle. Time for total on each stage of lavage cycle is expressed as a mean ± SD. Instilling time (stage a) is mean time (s) required for instilling saline into the lung. Retaining time (stage b) is mean time (s) applied for retaining saline in the lung. Draining time (stage c) is mean time (s) required for draining lavage fluid to the container. Preparing time (stage d) is mean time (s) required for preparation for the next saline instillation. †Each cycle time is the mean of stage a to d from 2nd to the last lavage. The 1st cycle required 120–1080 s. ‡Time (s) for the 1st 3 cycles ranged within 230–270 s, and that for the 4th to 11th cycles ranged within 625–680 s.

steeper than that for the right lung. The time required to reach 10% of the initial concentration of albumin in the first lavage was 2,730 s for the left lung, whereas it was 4,390 s for the right lung. Notably, both $K_S$ and $K_b$ of the left and right lungs were comparable ($1.77 \times 10^{-7}$ and $4.97 \times 10^{-10}$ cm/s, respectively, for the left lung; $1.60 \times 10^{-7}$ and $3.20 \times 10^{-10}$ cm/s, respectively, for the right lung).

When 1,000 ml of saline was assumed to be instilled into the lung in each cycle, the cumulative amount of albumin drained into the lavage fluid did not differ remarkably within retaining time of 90–570 s (Fig. 4*C*). The curve in short retaining time (90 s) slightly exceeded those in long retaining time (450–570 s) but reversed after 4,000 s. In this setting, the simulation impressed that ~3,200 s (53.3 min) would be required for enough elimination of albumin but that the efficiency of elimination would not significantly change after 5,400 s (90 min).

### *Effect of Instilled Saline Volume on the Efficiency of WLL*

*Eqs. 1–3* described in MATERIALS AND METHODS meant that the effect of WLL on elimination of proteins was affected by the instilled saline volume into the lung. As shown in Fig. 4*D*,

Table 4. *Volume balance during WLL*

| Case | Left/Right | First Cycle | | Second to the Last Cycle | | | |
|---|---|---|---|---|---|---|---|
| | | Instilled Volume, liters | Drained Volume, liters (recovery %) | Average Instilled Volume, liters | Average Drained Volume, liters (recovery %) | Total Instilled Volume, liters | Total Drained Volume, liters (recovery %) |
| 1 | L | 1.70 | 1.05 (61.8) | 0.96 | 0.93 (96.6) | 20.0 | 18.7 (93.7) |
| | R | 1.90 | 1.10 (57.9) | 1.04 | 1.01 (97.1) | 12.3 | 10.1 (82.1) |
| 2 | L | 1.40 | 0.50 (35.7) | 0.55 | 0.51 (91.4) | 11.9 | 10.1 (84.9) |
| | R | 1.50 | 0.90 (60.0) | 0.84 | 0.81 (96.6) | 17.5 | 16.4 (93.5) |
| 3 | L | 1.50 | 1.00 (66.7) | 0.85 | 0.82 (96.3) | 16.9 | 16.6 (93.8) |
| | R | 1.70 | 0.90 (52.9) | 0.88 | 0.89 (100.3) | 18.5 | 17.8 (95.9) |
| 4 | L | 0.90 | 0.37 (41.1) | 0.64 | 0.63 (97.1) | 16.5 | 14.7 (89.3) |
| | R | 1.40 | 1.00 (71.4) | 0.96 | 0.93 (97.0) | 28.2 | 27.0 (95.7) |
| 5 | L | 0.60 | 0.15 (25.0) | 0.49 | 0.46 (94.2) | 9.90 | 8.91 (90.0) |
| | R | 1.00 | 0.32 (32.0) | 0.59 | 0.56 (95.4) | 12.2 | 11.0 (90.2) |
| 6 | L | 1.00 | 0.60 (60.0) | 0.55 | 0.53 (96.6) | 11.4 | 10.7 (93.4) |
| | R | 1.00 | 0.50 (50.0) | 0.63 | 0.61 (95.8) | 13.0 | 12.0 (92.3) |
| 7 | R | 1.00 | 0.50 (50.0) | 0.76 | 0.75 (98.6) | 15.5 | 14.8 (95.5) |
| 8 | L | 1.10 | 0.27 (24.3) | 0.94 | 0.85 (89.7) | 15.2 | 13.0 (85.0) |
| | R | 1.30 | 0.47 (36.0) | 0.97 | 0.95 (98.5) | 19.8 | 18.5 (94.4) |
| 9 | L | 1.80 | 0.93 (51.9) | 1.58 | 1.48 (93.8) | 17.6 | 15.7 (89.5) |
| | R | 2.30 | 1.28 (55.7) | 1.94 | 1.90 (97.8) | 25.6 | 24.0 (94.1) |

The instilling volume of the 1st cycle in case 1–7 was determined by the following equations: functional residual capacity (ml) × 0.45 or 0.55 + tidal volume for the left and right lung, respectively. In case 8 and 9, saline was allowed to be instilled into the lung as much as possible from a bottle at 30 cm height from the tracheal tube.

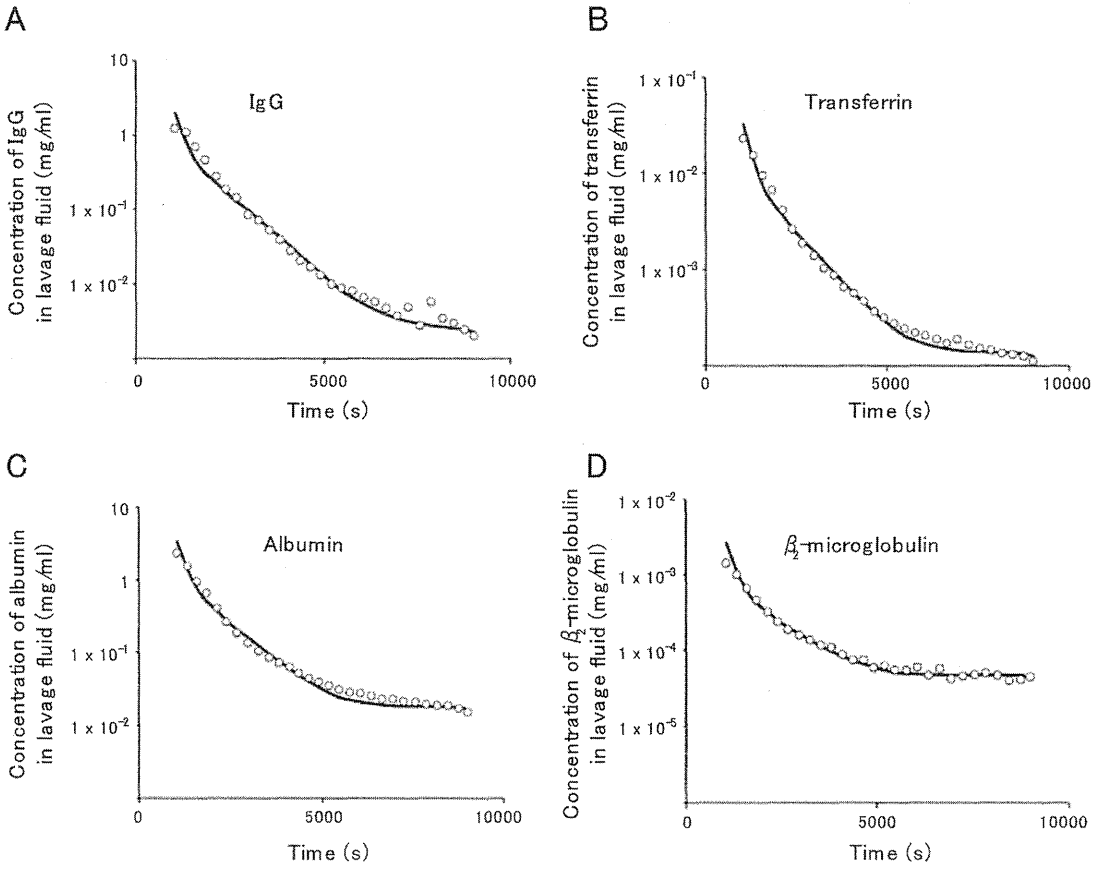


Fig. 2. Theoretical concentrations (lines) and measured concentration (plots) of IgG (*A*), transferrin (*B*), albumin (*C*), and $\beta_2$-microglobulin (*D*) in the drained aliquot of lavage fluid for each cycle. The vertical axis is the concentration of the protein on a log scale, and the horizontal axis indicates the time after the beginning of WLL.

when the cumulative eliminated albumin in case 1 was estimated in silico with fixed lavage cycle time at 240 s, the eliminated albumin appeared to increase as the instilled volume increased during 0 to ~3,200 s. After 3,200 s, the eliminated albumin gradually increased, but the volume effect seemed to be diminished.

### *Exceptional Substances That Fail to Follow the Mathematical Model*

Although we applied our mathematical model to the transfer of various substances during WLL, we found that the following substances did not follow the model.

*Gastrin and urea.* Measured levels of gastrin and urea did not exhibit an exponential decreasing phase but instead reached a plateau in the early stage of WLL (Fig. 5, *A* and *B*). Thus calculation of $K_s$ was difficult. Permeation of gastrin and urea from the blood to the lavage fluid occurred so quickly that the theoretical curves were hardly matched with the actual measurements, which themselves fluctuated markedly during the plateau phase.

*SP-D.* The SP-D concentration in the drained lavage fluid decreased consistently to a minor extent in the four lungs in the absence of an exponential phase and quickly reached a plateau in the early phase (Fig. 5*C*). As alveolar type II cells and nonciliated Clara cells abundantly release SP-D into the lower respiratory tract, this early plateau phase reflects its active release in situ.

*GM-CSF autoantibody.* Although the quantified GM-CSF autoantibody belongs to an IgG isotype, theoretical curves of the concentration in the drained lavage fluid did not fit with the measured autoantibody concentration even upon substitution of various sets of coefficients with $K_s$ and $K_b$ in all 17 lungs (Fig. 5*D*).

## DISCUSSION

By using a mathematical model based on measured concentrations of proteins, this study investigated the transfer of proteins from the surfactant and blood into the lavage fluid during WLL. We confirmed that the transfer followed a time-dependent differential equation, which assumes that the rate of transfer is proportional to the transmission coefficient, the effective surface area, and the protein gradient between the body compartment and lavage fluid (44).

By using various methods (e.g., comparisons of the protein concentrations between the plasma, sputum, and BALF) and by proving that the IgG1/IgG2 ratio between the BALF and serum are comparable, previous studies demonstrated the transfer of circulating proteins into the alveolar spaces (2, 14, 18, 28, 39).

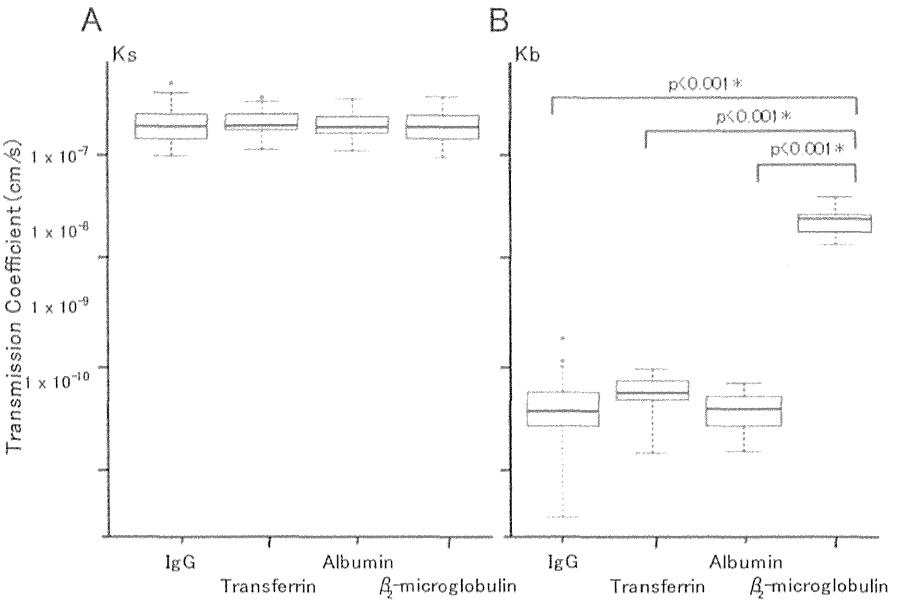


Fig. 3. Coefficients of transfer of IgG, transferrin, albumin, and $\beta_2$-microglobulin from surfactant ($K_s$) (*A*) and blood ($K_b$) (*B*) to the lavage fluid. The vertical axis indicates the transmission coefficients (cm/s) on a log scale. Statistical significance of coefficients between 2 proteins are shown in the figure.

More recently, intravenously injected GM-CSF autoantibodies were detected in the BALF of nonhuman primates and were observed to reproduce PAP (35). These results indicate that the antibody can cross the air-blood barrier (35). The kinetics of transfer from the blood to the air space and vice versa was studied both in vitro and in vivo (3, 23, 26, 27, 34). In one study, the transmission coefficient ($10^{-7}$-$10^{-5}$ cm/s) of various proteins across a monolayer of A549 cells was shown to indicate bidirectional transfer. These coefficients appear to be inversely correlated with the molecular weight of proteins (22). In another study, the transmission coefficient for proteins in a monolayer of rat alveolar epithelial cells in vitro was within $10^{-9}$-$10^{-7}$ cm/s, whereas that for albumin in sheep lung in vivo was $5 \times 10^{-10}$ cm/s (11, 17). Thus mass transfer from the blood to the air spaces may be continuously taking place even at steady state.

In previous studies by Ikegami et al. (15), surface tension maintained by surfactant materials covering the alveolar surface was found to have a probable role in interfering with massive transfer and subsequent accumulation of circulating proteins in the air spaces. Interference with the transfer is known to be disrupted by the elimination or deficiency of SP-B (15, 16). Lung lavage may remove surface-active materials in the alveoli and thus temporally disrupt the mechanisms that interfere with the influx of circulating proteins. It is for this reason that we focused on WLL to clarify the mechanism of protein transfer from the blood or surfactant to the lavage fluid. We found that the protein transfer followed a time-dependent mathematical model that was made analogous to the heat transmission model. To our knowledge, this is the first study that has clarified the mechanism of protein transfer in the lung during WLL.

To postulate a mathematical model, we assumed that the transfer of proteins from each body compartment to the lavage fluid consists of two pathways, namely transfer from the accumulated surfactant to the lavage fluid and transfer from the blood to the lavage fluid. The latter may be further divided into two pathways, namely transfer from the blood through the surfactant and direct transfer to the lavage fluid. However, we did not distinguish between these two latter pathways in this study because the transfer of a protein across the air-blood barrier seemed to be rate limiting. We found that protein transfer from the surfactant to the lavage fluid appeared to have $K_s$ values independent of the molecular weight and other properties. It is notable that the $K_s$ values did not differ among patients, indicating the reproducibility of the model. However, mass transfer from the blood to the lavage fluid with variable $K_b$ values did appear to be affected by the molecular weight of the protein because the protein was transferred through a semipermeable membrane consisting of endothelial cells, basement membrane, and type I pneumocytes. Transcytosis was proposed as the primary mechanism of protein transfer for large molecules and of partial paracellular diffusion of small molecules (7, 23). However, the true mechanism remains controversial. As indicated in this study, transfer of $\beta_2$-microglobulin (molecular weight of 11 kDa) from the blood to the lavage fluid had $K_b$ values that were two orders of magnitude higher than those of albumin, transferrin, and IgG, which had molecular weights of 66, 80, and 150 kDa, respectively. This difference suggests that $\beta_2$-microglobulin diffusion possesses a mechanism that is different from that of other proteins, i.e., it is supposed to be mainly transcytosis for albumin, transferrin, and IgG but mainly paracellular diffusion for $\beta_2$-microglobulin. Further analyses will be required to clarify the mechanisms by measuring the permeability of various substances with molecular weight of 10–60 kDa to confirm a "gap" in permeability coefficient $K_b$ among substances with molecular weights in this range.

It is notable that the decrease in concentrations of low-molecular-weight substances in the lavage fluid, namely urea (molecular weight of 60 kDa) and gastrin (molecular weight of 2.1 kDa), was inconsistent with our mathematical model. The measured concentrations appeared to fluctuate and appeared to be independent of time. Moreover, the phase of exponential

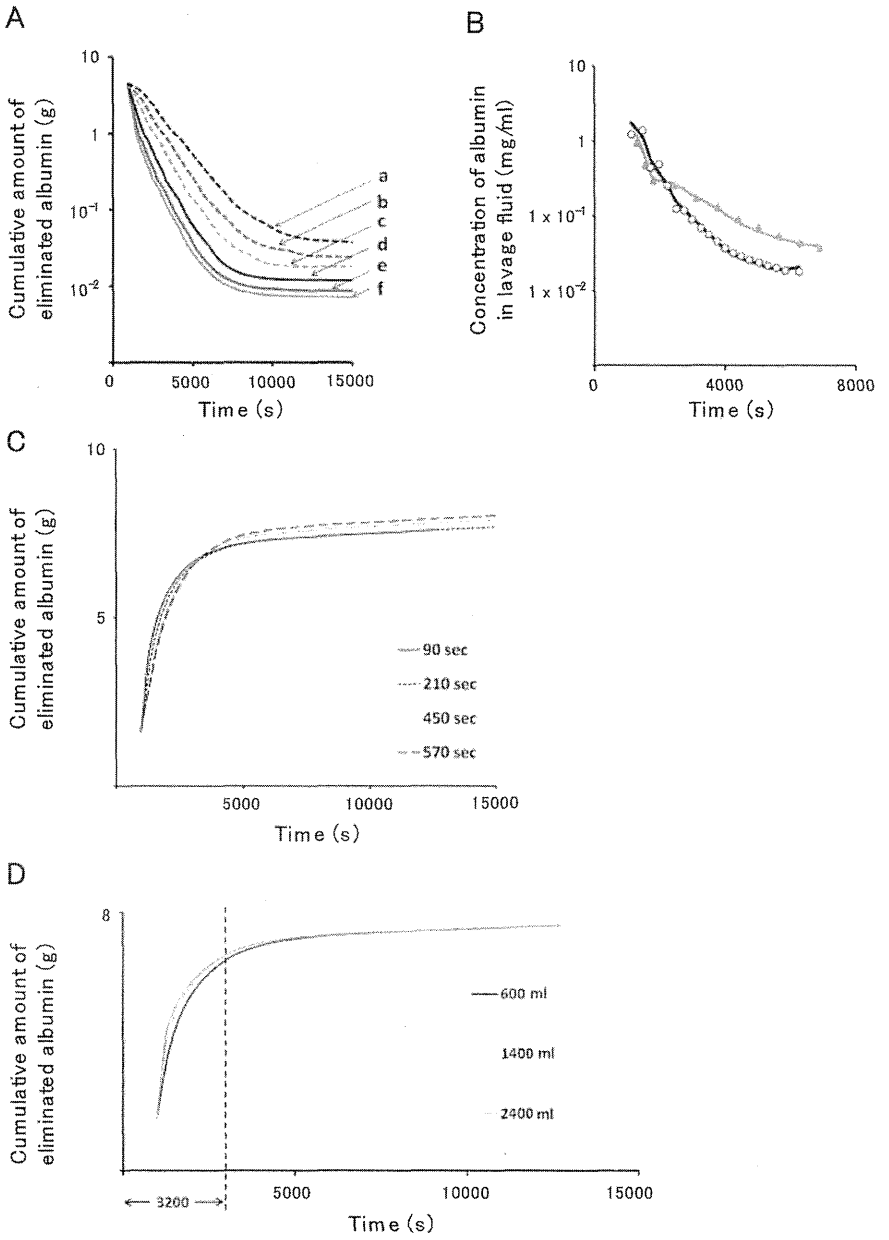


Fig. 4. *A*: durable effect of the retaining stage in each lavage cycle on the theoretical decreasing curve of albumin concentration in the drained lavage fluid. The time assumed for the retaining stage was variable: *a*, 540 s; b, 360 s; *c*, 240 s; *d*, 120 s; *e*, 60 s; and *f*, 30 s. The vertical axis indicates the albumin concentration in the lavage fluid (mg/ml). The horizontal axis indicates the time after the beginning of WLL. *B*: theoretical (lines; black, left; gray, right) and measured (plots: ⧠, left, ⧠, right) concentrations of albumin in the drained lavage fluid in each cycle. The vertical axis indicates the albumin concentration in the lavage fluid (mg/ml). The horizontal axis indicates the time after the beginning of WLL. *C*: simulation curves of cumulative amount of albumin drained in the drained lavage fluid when the retaining time varied with 90 (solid line), 210(small dashed line), 450(dotted line), or 570(large dashed line) s. *D*: cumulative amount of eliminated albumin in the drained lavage fluid. An in silico evaluation by changing instilled saline volume varied with 600 (black solid line), 1,400 (dotted line), or 2,400 (gray solid line) ml.

decrease was hardly defined in six out of ten lungs examined; when there was any decrease, the phase lasted within 1,000 s after the start of WLL (data not shown). This characteristic was likely due to the high permeability of the air-blood barrier to the molecules. Similarly, Rennard et al. (32) reported that urea was more able than glucose and albumin to permeate into the lavage fluid, as observed in normal volunteers with saline instilled into their lung segments.

SP-D is produced by alveolar type II cells and nonciliated Clara cells in the lower respiratory tracts and is secreted into the air space (43). Although SP-D is detectable in the sera of patients with aPAP, its levels are much lower than those of BAL (12). Thus SP-D transfer from the blood to the air space is negligible. The high concentration of SP-D in the lavage fluid was likely due to its continuous production in the lung. The rate of its production was estimated to be 6–13 mg/h on the basis of evaluation of four lungs (data not shown).

The lung is the organ that most abundantly produces GM-CSF, a factor that is critical for terminal differentiation of alveolar macrophages, as it promotes the expression of the transcription factor, PU.1 (38). It is suggested that IgG-type GM-CSF autoantibody is pathogenic and is known to be transferred from the lung capillaries into the air spaces immediately formed by GM-CSF autoantibody complex to become undetectable by our GM-CSF autoantibody ELISA system (30).

Furthermore, we had better to reconsider the adequacy of the present mathematical model when it was applied to substances

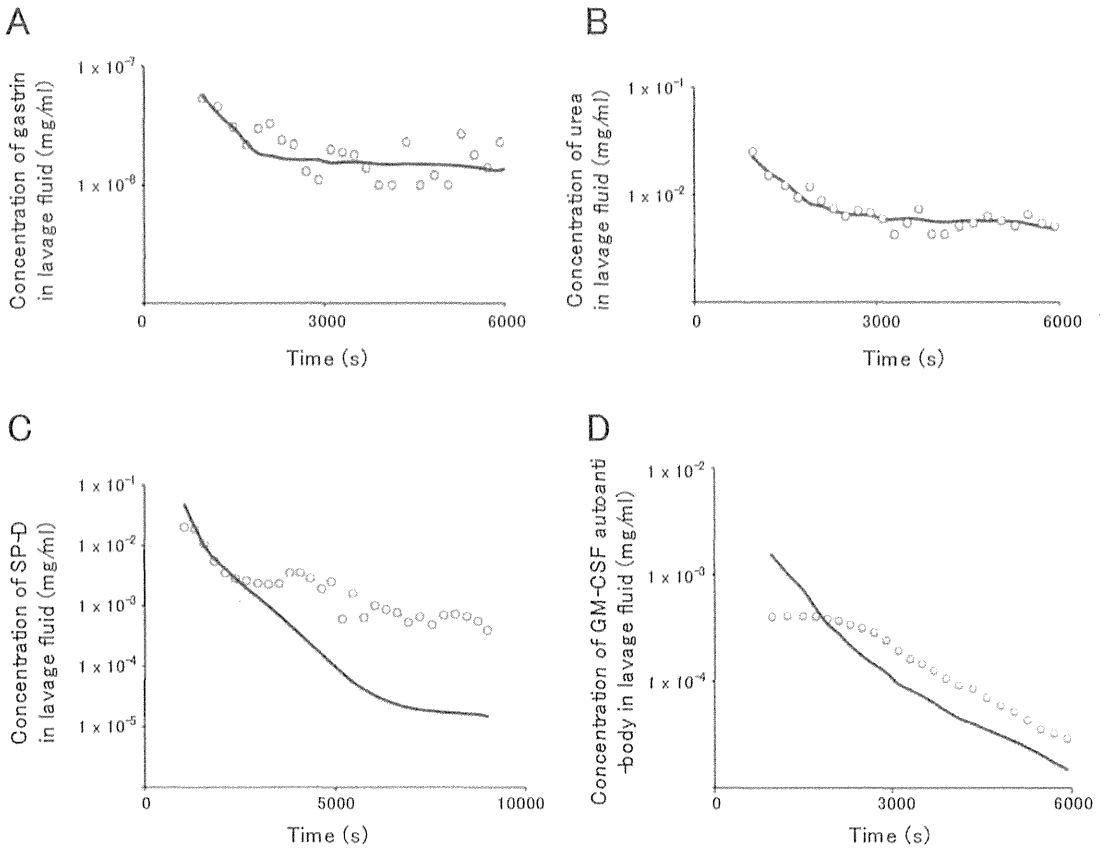


Fig. 5. *A* and *B*: actual measurements (plots) of gastrin or urea concentration in the drained lavage fluid did not exhibit the exponential decreasing phase but reached a plateau fluctuating in the early term. These seemed to migrate immediately from the blood to the lavage fluid. Thus the theoretical curves (lines) were hardly fitted with the actual measured concentration. *C*: concentration of surfactant protein D (SP-D) in the drained lavage fluid revealed slight decrease without exponential phase and soon reached a plateau phase in the early term. As SP-D is abundantly released from alveolar type II cells into the lower respiratory tracts, this early plateau phase probably reflected the active release in situ. *D*: actually measured granulocyte/macrophage colony-stimulating factor (GM-CSF) autoantibody concentrations were consistently under the theoretical curve especially in the early stage.

with lower molecular weights by assuming two permeation coefficients, such as $K_{b1}$ (coefficients from the blood to the lavage fluid through surfactant) and $K_{b2}$ (from the blood directly to the lavage fluid).

In the present study, the recovery rate in the first draining lavage fluid was lower than those after the second lavage. Although the first instilled saline remained in the lower respiratory tracts, we did not mind the remaining volume at the first draining because we thought that the remaining lavage fluid could be recovered after the second draining. Therefore, we did not intentionally extend the first draining time longer than those of other cycles. Although we usually perform percussion or vibration on the patient's chest, the recovery rate at the first draining was not improved by these procedures. It is likely that the low recovery rate and its variability of the first lavage shown in Table 4 were due to the early cessation of the first draining.

To date, methods of WLL for the treatment of PAP have not been standardized (25). Michaud et al. (29) recommended instilling 1 l of saline into the lavage lung and then to clamp the draining tube for 4–5 min (29). Bonella et al. (4) and Paschen et al. (31) determined the number of lavage cycles by measuring the optical density of each lavage fluid. They applied statistical evaluation to data from a number of WLLs to find the relationship between instilled saline volume and eliminated proteins. Although their approach is fundamentally different from ours, their finding that instilling volume is an important element for determining the amount of eliminated protein was confirmed in this study (Fig. 4*D*). The protocol for WLL used in this study were variable among participating hospitals, and thus time of each cycle varied between 213–630 s, including 120–540 s for the retaining time. As for our mathematical model, the number of cycles and the retaining times did not influence the efficiency of WLL. Based on *Eq. 1*, the amount of proteins eliminated by WLL was dependent on time after the beginning. According to the volume effect demonstrated by in silico simulation in this study (Fig. 4*D*), larger instilled volume appeared to improve the efficiency of lavage. However, the simulation also suggested that the effect is limited within some range of time. Previous studies, however, demonstrated the volume effect (4). In this regard, total eliminated albumin concentration significantly correlated with instilling saline volume in actually measured values in 17 WLLs of the present study with Rho value at 0.69. However, we have to consider the possibility that it also prolonged the duration of instilling and draining time, and thus longer time for each lavage cycle increases the elimi-

nated protein(s). Thus our mathematical model may be useful to predict the amount of eliminated proteins at a certain time point after the beginning of WLL.

In conclusion, we demonstrated that protein transfer in the lung during WLL followed a relatively simple, mathematical model based on diffusion and that this model could be expressed in terms of a number of differential equations. As an exception of the present mathematical model, substances with low molecular weight do not follow the theory. Our study, not only contributes to the design of an efficient regimen for WLL, but also reveals the mechanism of delivery of specific large drug molecules across the air-blood barrier, such as antibody drugs.

## APPENDIX

### *The Effective Alveolar Surface Area*

The effective alveolar surface area was calculated from the data for the alveolar volume, $V_A$ according to the following equations: $A_s = 6.4 \cdot 10^3 \cdot V_A^{2/3}$. For a person with 74 kg body wt, both $A_s$ and $V_A$ were reported to be 143 $m^2$ and 3,338 ml, respectively (10). The effective surface area of the pulmonary capillaries, $A_b$, was estimated from the following formula (10): $A_b = 0.89 \cdot A_s$. The relationship between alveolar surface area, $S_A$, and alveolar volume, $V_A$, depends on the number of alveoli. $S_A$ increases as the number of alveoli increases at a fixed value of $V_A$. According to Ref. 10, the average lung volume is 4,300 ml, and the average alveolar surface is $(143 \pm 12) \times 10^4$ $cm^2$ in normal subjects with an average body weight of 74 kg at 19–40 yr of age. Under these conditions, air-space volume density is $0.865 \pm 0.013$ $cm^2/cm^3$, and alveolar surface density is $370.6 \pm 28.9$ $cm^2/cm^3$.

We set

$$\beta = \frac{S_A^{\frac{1}{2}}}{V_A^{\frac{1}{3}}} \qquad (A1)$$

where, the right side of the equation is an expression for the constant shape parameter, β.

According to the report described above ($V_A$ and $S_A$ in the space V)

$$\frac{S_A}{V} = 370.6 \text{ cm}^2/\text{cm}^3 \qquad (A2)$$

$$S_A = 143 \times 10^4 \text{ cm}^2 \qquad (A3)$$

$$\frac{V_A}{V} = 0.865 \text{ cm}^3/\text{cm}^3 \qquad (A4)$$

From *Eqs. A2* and *A3*,

$$V = 3859 \text{ ml} \qquad (A5)$$

and from *Eqs. A4* and *A5*

$$V_A = 3338 \text{ ml} \qquad (A6)$$

where the anatomical dead space is 4,300 − 3,338 = 962 ml. Introducing *Eqs. A3* and *A6* into *Eq. A1*,

$$\beta = \frac{\sqrt{143 \times 10^4}}{\sqrt[3]{3338}} = 80.02 \qquad (A7)$$

On the basis of *Eq. A1* (note that $S_A$ is in $m^2$ and $V_A$ is in ml),

$$S_A = \beta^2 \cdot V_A^{\frac{2}{3}} = 6.403 \times 10^3 \cdot V_A^{\frac{2}{3}} \qquad (A8)$$

The value of β may be considered as constant even with a change in $V_A$ in the same subject, as the number of alveoli and the shape do not change, particularly in the supine position.

### *Method for Optimizing the Transmission Coefficients*

A program was written in Visual Basic Application using various coefficients to calculate the theoretical substance concentrations in the lavage aliquots. For explanation, we show an example of simulation used to obtain the best fitting curve shown in Fig. 2*C*. As shown in Appendix Fig. A1*A*, the value for $K_s$ could be determined to be $1.8 \times 10^{-7}$ cm/s by the least-square method until 3,000 s when $K_b$ was assumed to be 0 cm/s. Next, $K_b$ value was determined to be $5.2 \times 10^{-10}$ cm/s again by the least-square method by 9,018 s. As shown in Appendix Fig. A1*B*, the theoretical curve appeared closer to the dotted actual measurements. Then $K_b$ was changed to $6.1 \times 10^{-10}$ cm/s manually, as shown in Appendix Fig. A1*C*; the theoretical curve

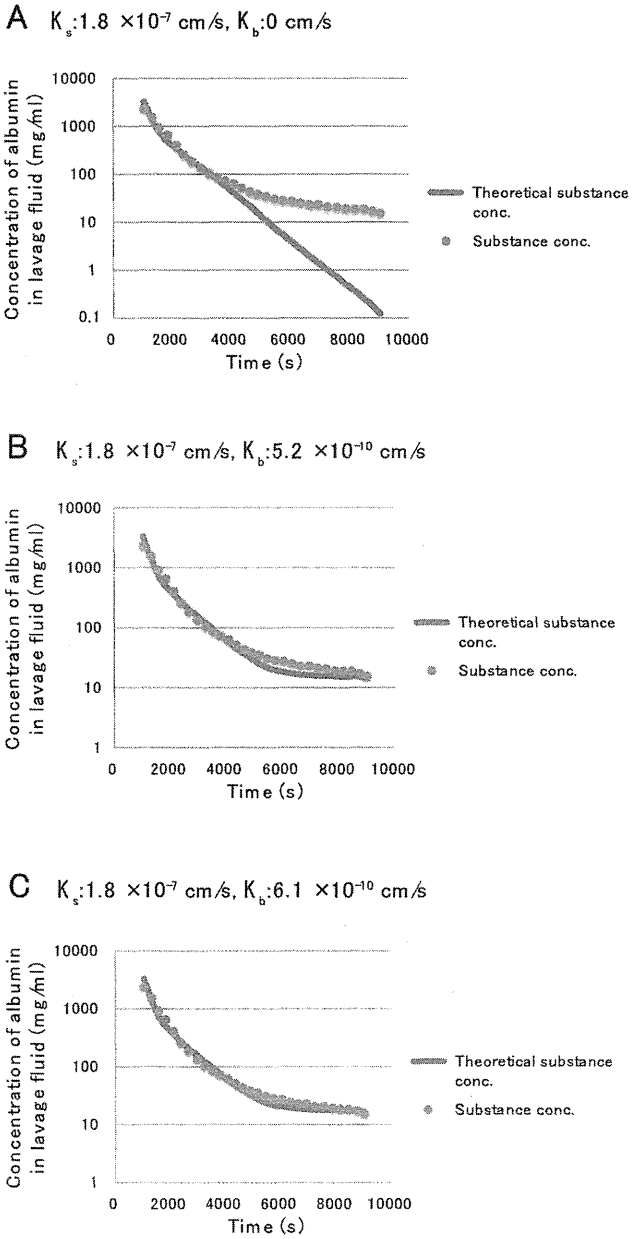


Fig. A1. Example of simulation used to obtain the best fitting curve shown in Fig. 2*C*.

completely coincides with the dotted actual measurements. Therefore, $K_b$ was determined to be $6.1 \times 10^{-10}$ cm/s.

## ACKNOWLEDGMENTS

The authors thank the investigators and patients for participating in this study. We also thank Dr. Matthew Sleeman and Dr. Tamiko Takemura for valuable discussions. We appreciate Ms. Marie Mori and Ms. Risako Seki for help in preparation of the manuscript and Ms. Kaoru Akasaka for schematic figure design. We thank Dr. Yasutsugu Fukushima, Dr. Naoto Fueki, Dr. Kiyokazu Kikuchi, Dr. Ryosuke Souma, Dr. Hideyuki Sato, Dr. Shingo Tokita, Dr. Kentaro Nakano, Dr. Yoichiro Mitsuishi, Dr. Ryoko Suzuki, and Dr. Takuro Sakagami for clinical contributions.

## GRANTS

This work was partly supported by a grant from Category B24390208 (K. Nakata), B12023059 (K. Nakata), and B24406027 (Y. Inoue) from the Japan Society for the Promotion of Science. This research was also supported by a grant from the Ministry of Health, Labour, and Welfare H24-Nanchi-Ippan-035 (Y. Inoue), H24 Rinken Sui-003 (R. Tazawa), and H26-Itaku(Nan)-Ippan-077 (Y. Inoue).

## DISCLOSURES

No conflicts of interest, financial or otherwise, are declared by the authors.

## AUTHOR CONTRIBUTIONS

K.A., T.M., K.U., R.T., T.I., Y. Inoue, and K.N. conception and design of research; K.A., A.H., Y. Ito, H.W., T.W., Takero Arai, H.M., S.O., R.T., T. Takada, E.Y., T.I., M. Hirose, and Toru Arai performed experiments; K.A., T. Tanaka, T.M., N.K., M. Hayashi, M. Hirose, and K.N. analyzed data; K.A., T. Tanaka, T.M., N.K., R.T., E.Y., H.K., and K.N. interpreted results of experiments; K.A., T. Tanaka, R.T., and K.N. prepared figures; K.A., T. Tanaka, T.M., K.U., T.I., and K.N. drafted manuscript; K.A., T.M., K.U., R.T., Toru Arai, H.K., and K.N. edited and revised manuscript; K.A., T. Tanaka, T.M., N.K., A.H., H.W., Takero Arai, M. Hayashi, H.M., K.U., S.O., R.T., T. Takada, E.Y., T.I., M. Hirose, Toru Arai, Y. Inoue, H.K., and K.N. approved final version of manuscript.

## REFERENCES

1. **Beccaria M, Luisetti M, Rodi G, Corsico A, Zoia MC, Colato S, Pochetti P, Braschi A, Pozzi E, Cerveri I.** Long-term durable benefit after whole lung lavage in pulmonary alveolar proteinosis. *Eur Respir J* 23: 526–531, 2004.
2. **Bernaudin JF, Bellon B, Pinchon MC, Kuhn J, Druet P, Bignon J.** Permeability of the blood-air barrier to antiperoxidase antibodies and their fragments in the normal rat lung. *Am Rev Respir Dis* 125: 734–739, 1982.
3. **Berthiaume Y, Albertine KH, Grady M, Fick G, Matthay MA.** Protein clearance from the air spaces and lungs of unanesthetized sheep over 144 h. *J Appl Physiol* 67: 1887–1897, 1989.
4. **Bonella F, Bauer PC, Griese M, Wessendorf TE, Guzman J, Costabel U.** Wash-out kinetics and efficacy of a modified lavage technique for alveolar proteinosis. *Eur Respir J* 40: 1468–1474, 2012.
5. **Campo I, Kadija Z, Mariani F, Paracchini E, Rodi G, Mojoli F, Braschi A, Luisetti M.** Pulmonary alveolar proteinosis: Diagnostic and therapeutic challenges. *Multidiscip Respir Med* 7: 4, 2012.
6. **Carey B, Trapnell BC.** The molecular basis of pulmonary alveolar proteinosis. *Clin Immunol* 135: 223–235, 2010.
7. **Conhaim RL, Watson KE, Lai-Fook SJ, Harms BA.** Transport properties of alveolar epithelium measured by molecular hetastarch absorption in isolated rat lungs. *J Appl Physiol* 91: 1730–1740, 2001.
8. **DeFouw DO.** Ultrastructural features of alveolar epithelial transport. *Am Rev Respir Dis* 127: S9–S13, 1983.
9. **Delacroix DL, Marchandise FX, Francis C, Sibille Y.** Alpha-2-macroglobulin, monomeric and polymeric immunoglobulin A, and immunoglobulin M in bronchoalveolar lavage. *Am Rev Respir Dis* 132: 829–835, 1985.
10. **Gehr P, Bachofen M, Weibel ER.** The normal human lung: Ultrastructure and morphometric estimation of diffusion capacity. *Respir Physiol* 32: 121–140, 1978.
11. **Gorin AB, Stewart PA.** Differential permeability of endothelial and epithelial barriers to albumin flux. *J Appl Physiol Respir Environ Exercise Physiol* 47: 1315–1324, 1979.
12. **Hartl D, Griese M.** Surfactant protein D in human lung diseases. *Eur J Clin Invest* 36: 423–435, 2006.
13. **Hastings RH, Folkesson HG, Matthay MA.** Mechanisms of alveolar protein clearance in the intact lung. *Am J Physiol Lung Cell Mol Physiol* 286: L679–L689, 2004.
14. **Huaringa AJ, Leyva FJ, Glassman AB, Haro MH, Arellano-Kruse A, Kim EE.** The lung permeability index: A feasible measurement of pulmonary capillary permeability. *Respir Med* 105: 230–235, 2011.
15. **Ikegami M, Weaver TE, Grant SN, Whitsett JA.** Pulmonary surfactant surface tension influences alveolar capillary shape and oxygenation. *Am J Respir Cell Mol Biol* 41: 433–439, 2009.
16. **Ikegami M, Whitsett JA, Martis PC, Weaver TE.** Reversibility of lung inflammation caused by SP-B deficiency. *Am J Physiol Lung Cell Mol Physiol* 289: L962–L970, 2005.
17. **Inoue Y, Trapnell BC, Tazawa R, Arai T, Takada T, Hizawa N, Kasahara Y, Tatsumi K, Hojo M, Ichiwata T, Tanaka N, Yamaguchi E, Eda R, Oishi K, Tsuchihashi Y, Kaneko C, Nukiwa T, Sakatani M, Krischer JP, Nakata K, Japanese Center of the Rare Lung Diseases Consortium.** Characteristics of a large cohort of patients with autoimmune pulmonary alveolar proteinosis in Japan. *Am J Respir Crit Care Med* 177: 752–762, 2008.
18. **Kim KJ, Malik AB.** Protein transport across the lung epithelial barrier. *Am J Physiol Lung Cell Mol Physiol* 284: L247–L259, 2003.
19. **Kim KJ, Matsukawa Y, Yamahara H, Kalra VK, Lee VH, Crandall ED.** Absorption of intact albumin across rat alveolar epithelial cell monolayers. *Am J Physiol Lung Cell Mol Physiol* 284: L458–L465, 2003.
20. **Kitamura T, Tanaka N, Watanabe J, Uchida Kanegasaki S, Yamada Y, Nakata K.** Idiopathic pulmonary alveolar proteinosis as an autoimmune disease with neutralizing antibody against granulocyte/macrophage colony-stimulating factor. *J Exp Med* 190: 875–880, 1999.
21. **Kitamura T, Uchida K, Tanaka N, Tsuchiya T, Watanabe J, Yamada Y, Hanaoka K, Seymour JF, Schoch OD, Doyle I, Inoue Y, Sakatani M, Kudoh S, Azuma A, Nukiwa T, Tomita T, Katagiri M, Fujita A, Kurashima A, Kanegasaki S, Nakata K.** Serological diagnosis of idiopathic pulmonary alveolar proteinosis. *Am J Respir Crit Care Med* 162: 658–662, 2000.
22. **Kobayashi S, Kondo S, Juni K.** Pulmonary delivery of salmon calcitonin dry powders containing absorption enhancers in rats. *Pharm Res* 13: 80–83, 1996.
23. **Kreyling WG, Hirn S, Möller W, Schleh C, Wenk A, Celik G, Lipka J, Schäffler M, Haberl N, Johnston BD, Sperling R, Schmid G, Simon U, Parak WJ, Semmler-Behnke M.** Air-blood barrier translocation of tracheally instilled gold nanoparticles inversely depends on particle size. *ACS Nano* 8: 222–233, 2014.
24. **Lee KN, Levin DL, Webb WR, Chen D, Storto ML, Golden JA.** Pulmonary alveolar proteinosis: high-resolution CT, chest radiographic, and functional correlations. *Chest* 111: 989–995, 1997.
25. **Luisetti M.** Call for an international survey on therapeutic lavage for pulmonary alveolar proteinosis. *Eur Respir J* 39: 1049, 2012.
26. **Matsukawa Y, Yamahara H, Yamashita F, Lee VH, Crandall ED, Kim KJ.** Rates of protein transport across rat alveolar epithelial cell monolayers. *J Drug Target* 7: 335–342, 2000.
27. **Matthay MA, Berthiaume Y, Staub NC.** Long-term clearance of liquid and protein from the lungs of unanesthetized sheep. *J Appl Physiol* 59: 928–934, 1985.
28. **Merrill WW, Naegel GP, Olchowski JJ, Reynolds HY.** Immunoglobulin G subclass proteins in serum and lavage fluid of normal subjects. Quantitation and comparison with immunoglobulins A and E. *Am Rev Respir Dis* 131: 584–587, 1985.
29. **Michaud G, Reddy C, Ernst A.** Whole-lung lavage for pulmonary alveolar proteinosis. *Chest* 136: 1678–1681, 2009.
30. **Nei T, Urano S, Motoi N, Takizawa J, Kaneko C, Kanazawa H, Tazawa R, Nakagaki K, Akagawa KS, Akasaka K, Ichiwata T, Azuma A, Nakata K.** IgM-type GM-CSF autoantibody is etiologically a bystander but associated with IgG-type autoantibody production in autoimmune pulmonary alveolar proteinosis. *Am J Physiol Lung Cell Mol Physiol* 302: L959–L964, 2012.
31. **Paschen C, Reiter K, Stanzel F, Teschler H, Griese M.** Therapeutic lung lavages in children and adults. *Respir Res* 6: 138, 2005.
32. **Rennard SI, Basset G, Lecossier D, O'Donnell KM, Pinkston P, Martin PG, Crystal RG.** Estimation of volume of epithelial lining fluid recovered by lavage using urea as marker of dilution. *J Appl Physiol* 60: 532–538, 1986.
33. **Rosen SH, Castleman B, Liebow AA.** Pulmonary alveolar proteinosis. *N Engl J Med* 258: 1123–1142, 1958.
34. **Ryan GM, Kaminskas LM, Kelly BD, Owen DJ, McIntosh MP, Porter CJ.** Pulmonary administration of PEGylated polylysine dendrimers: Ab-

sorption from the lung versus retention within the lung is highly size-dependent. *Mol Pharm* 10: 2986–2995, 2013.
35. **Sakagami T, Uchida K, Suzuki T, Carey BC, Wood RE, Wert SE, Whitsett JA, Trapnell BC, Luisetti M.** Human GM-CSF autoantibodies and reproduction of pulmonary alveolar proteinosis. *N Engl J Med* 361: 2679–2681, 2009.
36. **Selecky PA, Wasserman K, Benfield JR, Lippmann M.** The clinical and physiological effect of whole-lung lavage in pulmonary alveolar proteinosis: a ten-year experience. *Ann Thorac Surg* 24: 451–461, 1977.
37. **Seymour JF, Presneill JJ.** Pulmonary alveolar proteinosis: progress in the first 44 years. *Am J Respir Crit Care Med* 166: 215–235, 2002.
38. **Shibata Y, Berclaz PY, Chroneos ZC, Yoshida M, Whitsett JA, Trapnell BC.** GM-CSF regulates alveolar macrophage differentiation and innate immunity in the lung through PU.1. *Immunity* 15: 557–567, 2001.
39. **Stockley RA, Mistry M, Bradwell AR, Burnett D.** A study of plasma proteins in the sol phase of sputum from patients with chronic bronchitis. *Thorax* 34: 777–782, 1979.
40. **Trapnell BC, Whitsett JA, Nakata K.** Pulmonary alveolar proteinosis. *N Engl J Med* 349: 2527–2539, 2003.
41. **Uchida K, Nakata K, Carey B, Chalk C, Suzuki T, Sakagami T, Koch DE, Stevens C, Inoue Y, Yamada Y, Trapnell BC.** Standardized serum GM-CSF autoantibody testing for the routine clinical diagnosis of autoimmune pulmonary alveolar proteinosis. *J Immunol Methods* 402: 57–70, 2014.
42. **Uchida K, Nakata K, Trapnell BC, Terakawa T, Hamano E, Mikami A, Matsushita I, Seymour JF, Oh-Eda M, Ishige I, Eishi Y, Kitamura T, Yamada Y, Hanaoka K, Keicho N.** High-affinity autoantibodies specifically eliminate granulocyte-macrophage colony-stimulating factor activity in the lungs of patients with idiopathic pulmonary alveolar proteinosis. *Blood* 103: 1089–1098, 2004.
43. **Wright JR, Dobbs LG.** Regulation of pulmonary surfactant secretion and clearance. *Annu Rev Physiol* 53: 395–414, 1991.
44. **Yamashita AC.** Quantification of peritoneal transport. *Perit Dial Int*, 28 *Suppl* 3: S139–S143, 2008.

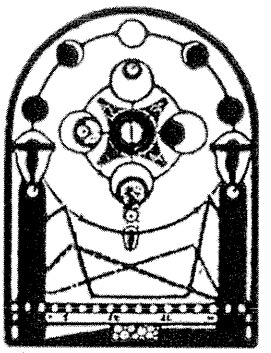

Cytokine 68 (2014) 118–126

Contents lists available at ScienceDirect

Cytokine

journal homepage: www.journals.elsevier.com/cytokine

# Low concentrations of recombinant granulocyte macrophage-colony stimulating factor derived from Chinese hamster ovary cells augments long-term bioactivity with delayed clearance *in vitro*

Atsushi Hashimoto [a], Takahiro Tanaka [a], Yuko Itoh [a], Akira Yamagata [b], Nobutaka Kitamura [c], Ryushi Tazawa [a], Kazuhide Nakagaki [d], Koh Nakata [a,*]

[a] *Bioscience Medical Research Center, Niigata University Medical and Dental Hospital, 1-754, Asahimachi-dori, Chuo-ku, Niigata 951-8510, Japan*
[b] *Towa Environment Science Co., Ltd. Prophoenix Division, 1-24-22 Nanko-kita, Suminoe, Osaka 559-0034, Japan*
[c] *Department of Medical Informatics, Niigata University Medical and Dental Hospital, 1-754, Asahimachi-dori, Chuo-ku, Niigata 951-8510, Japan*
[d] *Laboratory of Infectious Diseases and Immunology, College of Veterinary Medicine, Nippon Veterinary and Life Science University, 1-1-5, Sendagi, Bunkyo-ku, Tokyo 113-8602, Japan*

ARTICLE INFO

*Article history:*
Received 3 December 2013
Received in revised form 18 February 2014
Accepted 24 March 2014
Available online 9 May 2014

*Keywords:*
GM-CSF
TF-1 cells
CHO cells
Sialic acid
Oligosaccharide

ABSTRACT

To date, the biological activity of granulocyte macrophage-colony stimulating factor (GM-CSF) has been investigated by using mostly *Escherichia coli*- or yeast cell-derived recombinant human GM-CSF (erhGM-CSF and yrhGM-CSF, respectively). However, Chinese hamster ovary cell-derived recombinant human GM-CSF (crhGM-CSF), as well as natural human GM-CSF, is a distinct molecule that includes modifications by complicated oligosaccharide moieties. In the present study, we reevaluated the bioactivity of crhGM-CSF by comparing it with those of erhGM-CSF and yrhGM-CSF. The effect of short-term stimulation (0.5 h) on the activation of neutrophils/monocytes or peripheral blood mononuclear cells (PBMCs) by crhGM-CSF was lower than those with erhGM-CSF or yrhGM-CSF at low concentrations (under 60 pM). Intermediate-term stimulation (24 h) among the different rhGM-CSFs with respect to its effect on the activation of TF-1 cells, a GM-CSF-dependent cell line, or PBMCs was not significantly different. In contrast, the proliferation/survival of TF-1 cells or PBMCs after long-term stimulation (72–168 h) was higher at low concentrations of crhGM-CSF (15–30 pM) than that of cells treated with other GM-CSFs. The proportion of apoptotic TF-1 cells after incubation with crhGM-CSF for 72 h was lower than that of cells incubated with other rhGM-CSFs. These effects were attenuated by desialylation of crhGM-CSF. Clearance of crhGM-CSF but not desialylated-crhGM-CSF by both TF-1 cells and PBMCs was delayed compared with that of erhGM-CSF or yrhGM-CSF. These results suggest that sialylation of oligosaccharide moieties delayed the clearance of GM-CSF, thus eliciting increased long-term bioactivity *in vitro*.



## 1. Introduction

Granulocyte macrophage-colony stimulating factor (GM-CSF) is a hematopoietic growth factor that regulates the growth, differentiation, and maturation of myeloid precursor cells and promotes the function of mature neutrophils, eosinophils, and monocytes [1–4]. It elicits these diverse effects through interaction with a unique dodecameric receptor complex on cells, which consists of α and common β chains [5–7]. GM-CSF signaling induces phosphorylation of Janus kinase 2 (JAK2) and the common β chains, followed by activation of signal transducers and activators of transcription (STATs) [5,7,8]. Upon immune stimulation, it is produced by a variety of cell types, including T cells, macrophages, endothelial cells, and fibroblasts. Although GM-CSF is produced locally [3], it can

*Abbreviations:* ACN, acetonitrile; ANOVA, analysis of variance; CHO, Chinese hamster ovary; crhGM-CSF, CHO-derived recombinant human GM-CSF; erhGM-CSF, *Escherichia coli*-derived recombinant human GM-CSF; FCS, fetal calf serum; FITC, fluorescein isothiocyanate; GM-CSF, granulocyte macrophage-colony stimulating factor; JAK2, Janus kinase 2; MIP-1α, macrophage inflammatory protein; $NaN_3$, sodium azide; PBMCs, peripheral blood mononuclear cells; SDS-PAGE, sodium dodecyl sulfate–polyacrylamidegel electrophoresis; STAT5, signal transduction and activator of transcription; TFA, trifluoroacetic acid; TOF mass spectrometer, time-of-flight mass spectrometer; yrhGM-CSF, yeast cell-derived recombinant human GM-CSF.

* Corresponding author. Tel.: +81 25 227 0847.
*E-mail addresses:* noiredge2007@yahoo.co.jp (A. Hashimoto), belltatnk@gmail.com (T. Tanaka), y-itoh@med.niigata-u.ac.jp (Y. Itoh), yamagata@prophoenix.jp (A. Yamagata), nktmr@m12.alpha-net.ne.jp (N. Kitamura), ryushi@med.niigata-u.ac.jp (R. Tazawa), nakagaki@nvlu.ac.jp (K. Nakagaki), radical@med.niigata-u.ac.jp (K. Nakata).

http://dx.doi.org/10.1016/j.cyto.2014.03.009
1043-4666/

act in a paracrine fashion to recruit circulating neutrophils, monocytes, and lymphocytes to enhance their function in host defense [9,10]. GM-CSF is used clinically to prevent neutropenia and associated infections by promoting the proliferation of hematopoietic progenitor cells after chemotherapy, by promoting the differentiation of myeloid cells, and by enhancing the antibacterial activities of neutrophils and macrophages [10–14].

Natural human GM-CSF (hGM-CSF) has been purified from several sources, including medium conditioned with placenta cells or activated blood lymphocytes [15–19]. It is a glycoprotein that consists of 127 amino acid residues, with four cysteines involved in two disulfide bonds, forming a compact globular structure that comprises four α-helices joined by loops. It is found extracellularly as a homodimer [6,7] with two N-glycosylation sites at Asn27 and Asn37 and three O-glycosylation sites at Ser7, Ser9, and Thr10 [15]. The most heavily glycosylated hGM-CSF, with a molecular weight of 28–32 kDa, has two N-linked carbohydrate moieties, whereas the partially glycosylated hGM-CSF, with a molecular weight of 23–25 kDa, contains one N-linked carbohydrate moiety. A minimally glycosylated hGM-CSF with molecular weight of 16–18 kDa consists of only one O-linked carbohydrate [15,20].

Cells from various species can produce recombinant hGM-CSF (rhGM-CSF) [21,22]. However, only commercial preparations produced from *Escherichia coli* and *Saccharomyces cerevisiae* are available for clinical use. Commercial *E. coli*-derived recombinant hGM-CSF (erhGM-CSF), Molgramostim, is non-glycosylated, consists of 127 amino acid residues, has a molecular weight of 14.5 kDa, and is methylated at the N-terminal end [23]. Commercial *Saccharomyces*-derived recombinant hGM-CSF (yrhGM-CSF), Sargramostim, is a glycoprotein of 127 amino acids composed of three primary molecular species having molecular weights of 19.5, 16.8, and 15.5 kDa [23]. Its amino acid sequence differs from hGM-CSF by a substitution of leucine at position 23 [23]. On the other hand, rhGM-CSF derived from Chinese hamster ovary (CHO) cells (crhGM-CSF) has a molecular weight of 15–32 kDa with the same N-glycosylation and O-glycosylation sites as those of hGM-CSF, although the carbohydrate moieties added are probably different. Forno et al. demonstrated that the N-glycan terminal contains mono- and disialic acid residues, but has predominantly tri- or tetrasialic acid residues with and without N-acetyllactosamine repeat units. N-glycans contain more than 90% α-1,6-linked fucose at the proximal end [20].

The pattern of glycosylation on GM-CSF is known to affect its biological activity. Proliferation of a human monocytic leukemia cell line incubated with the heavily glycosylated hGM-CSF (28–32 kDa) was reduced six fold compared with proliferation after treatment with non-glycosylated erhGM-CSF, while neutrophil superoxide anion production was reduced by up to 10-fold. Partially glycosylated hGM-CSF (23–25 kDa) and minimally glycosylated hGM-CSF (16–18 kDa) have biological activity similar to that of erhGM-CSF. The binding capacity of these hGM-CSFs for the rhGM-CSF receptor on neutrophils decreases with increasing molecular weight [15]. Similarly, most studies on mammalian cell-derived, glycosylated GM-CSF (including crhGM-CSF) demonstrate that glycosylation of GM-CSF prolongs the *in vivo* half life by stabilizing the protein, but reduces its binding avidity to the GM-CSF receptor and decreases its biological activities such as colony-forming activity of bone marrow cells and neutrophil superoxide anion production [15,24].

In contrast to previous studies [15,24], we showed in the present study that glycosylated rhGM-CSF produced by CHO cells exhibited increased proliferation/survival of TF-1 cells, PBMCs and monocytes at low GM-CSF concentrations compared with that of erhGM-CSF and yrhGM-CSF *in vitro*. Desialylation of crhGM-CSF attenuated this effect, indicating that the sialyl residue is crucial for augmenting the long-term activity of GM-CSF. Moreover, we examined the mechanism of this effect by measuring the clearance of rhGM-CSF by cells.

## 2. Materials and methods

### 2.1. Material

#### 2.1.1. Cells

TF-1, a GM-CSF-dependent cell line, was kindly provided by Kitamura et al. [22].

Peripheral blood mononuclear cells (PBMCs) and monocytes were isolated from the peripheral blood of healthy donors as described previously [8]. Written informed consent was obtained under protocols approved by the institutional review boards of the Niigata University Medical Dental Hospital.

#### 2.1.2. rhGM-CSF

Molgramostim and Sargramostim were purchased from Amoytop Biotech Co., Ltd. (Xiamen, Fujian, PRC) and Genzyme Corporation (Cambridge, MA, USA), respectively. crhGM-CSF was kindly provided by JCR Pharmaceuticals Co., Ltd. (Ashiya, Hyogo, Japan).

#### 2.1.3. Desialylation of crhGM-CSF

crhGM-CSF (1 mg/ml) was incubated with neuraminidase agarose from *Clostridium perfringens* (0.05 U/ml, Sigma–Aldrich, MO, USA) in 100 mM sodium acetate buffer with $CaCl_2$ (pH 5.0) for 60 min at 37 °C. After the agarose was removed, the solution was dialyzed against PBS overnight at 4 °C.

### 2.2. Mass spectrometry

Protein (10 μl) was mixed with 90 μl of 0.1% trifluoroacetic acid (TFA) and 0.5 μl of MB-HIC8 magnetic C8 beads (Bruker Daltonics, Hercules, MA, USA) in a PCR tube and then incubated for 5 min at room temperature. The tube was subsequently placed in a magnetic beads separator and the supernatant was removed by using a pipette. The magnetic beads were then washed three times with 100 μl of 0.1% TFA. The bound proteins were eluted from the magnetic beads by using 4.5 μl of 60% acetonitrile (ACN) in 0.1% TFA. Two microliters of the eluate was mixed with 1 μl of matrix solution (10 g/l sinapinic acid in 70% ACN, 0.1% TFA) and was spotted on a polished steel plate. The mass spectra were obtained on an Ultraflex TOF/TOF mass spectrometer (Bruker Daltonics, Hercules, MA, USA) operated in positive-ion linear mode.

### 2.3. Phosphorylated STAT5 detection assay

Heparinized fresh whole blood was incubated with 15, 30, 60, or 500 pM rhGM-CSF, for 30 min at 37 °C and fixed, and then red blood cells were lysed in Fix/Lyse buffer (BD Biosciences, Franklin Lakes, New Jersey, USA) for 20 min at 37 °C. White blood cells were collected by centrifugation and fixed in ice-cold methanol at −20 °C for 1 h. After centrifugation, the cells were resuspended in 3% FCS/0.01% $NaN_3$/PBS solution and incubated with Alexa Fluor 647-labeled anti-pSTAT5 (BD Biosciences, San Jose, CA, New Jersey, USA). Cells with phosphorylated STAT5 in granulocytes/monocytes detected by flow cytometry (Cell Analyzer, Sony, Tokyo, Japan).

### 2.4. Neutrophil CD11b stimulation index assay

The neutrophil CD11b assay was performed as described previously [25]. Aliquots of heparinized fresh whole blood were incubated with rhGM-CSF, and cell-surface CD11b levels were quantified by flow cytometry (Sony, Tokyo, Japan). The CD11b

stimulation index was calculated as the mean fluorescent intensity of stimulated neutrophils minus the mean fluorescent intensity of unstimulated neutrophils divided by the mean fluorescent intensity of unstimulated neutrophils and multiplied by 100.

### 2.5. Measurement of GM-CSF-induced MIP-1α in PBMCs

To evaluate GM-CSF-induced MIP-1α production in normal PBMCs, $1 \times 10^6$ cells were incubated with or without GM-CSF in macrophage-serum-free medium (GIBCO BRL, Palo Alto, CA, USA). MIP-1α levels in the supernatant were measured by ELISA (Quantikine, R&D Systems, Mincapolis, MN, USA) according to the manufacturer's instructions [26].

### 2.6. Cell proliferation/survival assay

TF-1 cells, PBMCs and monocytes ($2 \times 10^4$ cells/well) were incubated with various concentrations of GM-CSF in macrophage serum free medium (GIBCO BRL, Palo Alto, CA, USA) for 3 and 7 days, respectively [27]. At the end of the incubation, 10 μl of 100 μl (5-[2,4-bis(sodiooxysulfonyl)phenyl-3-(2-methoxy-4-nitrophenyl)-2-(4-nitrophenyl)-2*H*-tetrazole-3-ium]) CCK-8, Doujindo, Kumamoto, Japan) was added to each well. Cells were further incubated at 37 °C under 5% $CO_2$ for 4 h, and formazan formation was measured as absorbance at 450 nm by using a microplate reader (Bio-Rad, CA, USA).

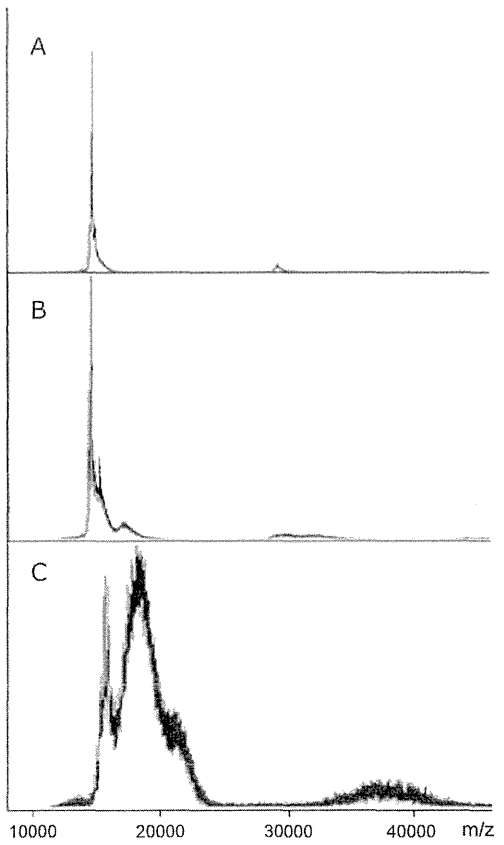


**Fig. 1.** Mass spectra of rhGM-CSFs. (A) *E. coli*-derived recombinant human GM-CSF. (B) Yeast-derived recombinant human GM-CSF. (C) CHO cell-derived recombinant human GM-CSF. The horizontal axis is the molecular weight (Da) and the vertical axis is the intensity.

### 2.7. Inhibition of TF-1 cell growth by antibodies

A cell proliferation/survival assay was performed in the presence or absence of 500 ng/ml goat anti-GM-CSF antibody (R&D Systems, Mincapolis, MN, USA), which was purified from the serum of a goat immunized with erhGM-CSF.

### 2.8. Morphology and cell-survival assay

TF-1 cells ($1 \times 10^5$ cells) incubated with rhGM-CSF were cytocentrifuged at 200 rpm for 2 min by using a Cytospin (Thermo Scientific, Waltham, MA, USA) and were then stained with Diff-Quick (Sysmex, Hyogo, Japan). The sizes of five hundred cells were measured under a high magnification field by using a micrometer (MeCan Imaging, Saitama, Japan). The percentage of living cells was determined by flow cytometry (Sony, Tokyo, Japan) using staining with propidium iodide solution (Annexin-V-FLUOS Staining Kit, Roche, Basel, Switzerland) according to the manufacturer's instructions.

### 2.9. SDS–PAGE

rhGM-CSFs (6.5 ng) were subjected to SDS–PAGE under reducing conditions. The gel was stained by using gel stain solution (ORIOLE Fluorescent Gel Stain, Bio-Rad, CA, USA), and the banding pattern was visualized under an image analyzer (MiniLumi, Berthold Technologies, Bad Wildbad, Germany).

### 2.10. Detection of apoptosis

#### 2.10.1. FITC-Annexin V preparation

TF-1 cells ($1 \times 10^6$ cells) were stained with FITC-labeled anti-Annexin-V antibody (Annexin-V-FLUOS Staining Kit, Roche,

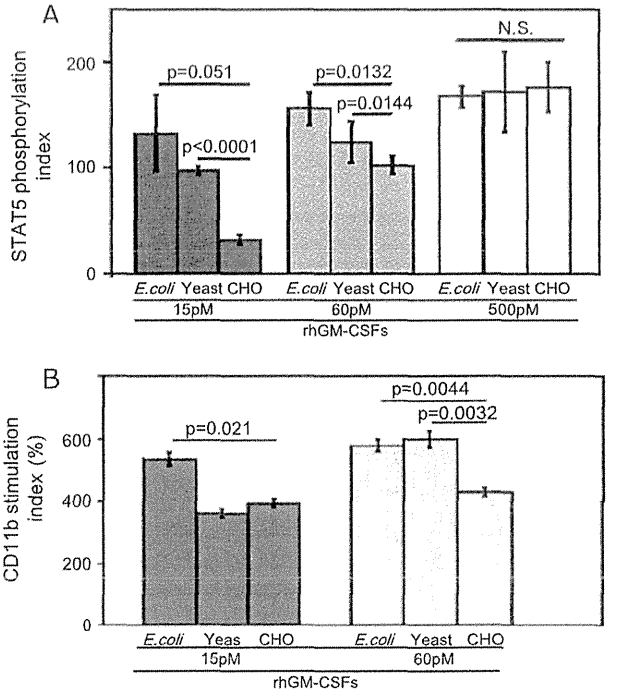


**Fig. 2.** Effect of short-term stimulation (0.5 h) by *E. coli*-, yeast-, and CHO cell-derived rhGM-CSF. The phosphorylation of STAT5 (A) and CD11b expression of neutrophils and monocytes (B). Whole blood cells were incubated for 0.5 h with 15, 60, or 500 pM of each rhGM-CSF for in (A) and 15 or 60 pM in (B). The vertical axis is STAT5 phosphorylation index (A) and CD11b stimulation index (B) is defined as described in Section 2.

Basel, Switzerland) for 15 min at 4 °C, and the stained cells were detected by flow cytometry (Sony, Tokyo, Japan). FITC-labeled mouse IgG isotype was used as the control.

*2.10.2. DNA fragmentation assay*

TF-1 cells ($2 \times 10^5$ cells/ml) were incubated with 15 pM of rhGM-CSF for 3 days [27].

At the end of the incubation, DNA was extracted from TF-1 cells by using a QIAamp DNA Mini Kit (QIAGEN, Valencia, CA, USA). DNA (3.5 μg) was loaded on 1% agarose gel and electrophoresed for 25 min at 100 V (constant voltage). After the gel was stained with ethidium bromide solution (10 mg/ml, Nippon Gene, Tokyo, Japan), the banding pattern was visualized under an image analyzer (Mini-Lumi, Berthold Technologies, Bad Wildbad, Germany).

*2.11. GM-CSF clearance assay*

GM-CSF clearance assay was performed as described previously [8]. To assess receptor-mediated binding and uptake of exogenous GM-CSF, $1 \times 10^6$ PBMCs or $4 \times 10^5$ TF-1 cells per well in a 24-well culture plate were incubated in RPMI 1640 (GIBCO BRL, Palo Alto, CA, USA) containing 10% FCS (Nichirei, Bioscience Inc, Tokyo, Japan) 100 mg/ml streptomycin and 100 U/ml penicillin under 5% $CO_2$ at 37 °C. rhGM-CSF was added at concentrations of 5 and 15 pM to PBMCs and TF-1 cells, respectively. The concentration of rhGM-CSF in the supernatant of each well was then measured at 5, 10, 24, and 48 h by ELISA.

*2.12. Statistical analysis*

Numerical data were evaluated for normal distribution by using Shapiro–Wilk tests. Parametric data are presented as means (±SE). Parametric data were analyzed by using one-way factorial ANOVA measurements. Multiple comparisons were performed through a Bonferroni-adjusted *t*-test, with non-significance set at $p > 0.05$. All tests were two-sided and *p* values <0.05 were considered statistically significant. Data were analyzed by using JMP (10.0.0) software (SAS, Cary, NC, USA).

## 3. Results

*3.1. Molecular weight of rhGM-CSF*

In this study, the bioactivity of rhGM-CSF derived from *E. coli*, yeast, and CHO cells was evaluated and compared. The mass spectrum of each GM-CSF shows distinct characteristic peaks: a single peak at 14.5 kDa for erhGM-CSF; peaks at 14.2, 14.4, and 15.0 kDa for yrhGM-CSF corresponding to a mean molecular weight of 14.7 kDa; and a number of peaks ranging from 16–28 kDa for crhGM-CSF corresponding to mean molecular weight of 19.0 kDa (Fig. 1A). The molar concentration of each rhGM-CSF was calculated from the original weight and volume, and then dividing by each mean molecular weight.

*3.2. Short-term biological activity of rhGM-CSF*

To compare the short-term bioactivity of the three rhGM-CSFs, we first evaluated the phosphorylation of STAT5 in monocytes and neutrophils stimulated for 0.5 h with the rhGM-CSFs. At both 15 and 60 pM rhGM-CSF, the percentage of pSTAT5-positive cells was significantly lower in crhGM-CSF-treated cells than in erhGM-CSF- or yrhGM-CSF-treated cells; whereas at 500 pM, this percentage was similar among the three rhGM-CSFs (Fig. 2A). Maximal values of CD11b stimulation indices at 60 pM of rhGM-CSF were 425 ± 15%, 576 ± 27%, and 625 ± 33%, for crhGM-CSF, erhGM-CSF, and yrhGM-CSF, respectively (Fig. 2B). These results indicate that the short-term effect of stimulation with crhGM-CSF was smaller than that with erhGM-CSF and yrhGM-CSF.

*3.3. Intermediate-term biological activity of rhGM-CSF*

When TF-1 cells were incubated with 30–120 pM rhGM-CSF for 24 h, the proliferation/survival was similar after treatment with crhGM-CSF, erhGM-CSF, and yrhGM-CSF (Fig. 3A). Likewise, MIP-1α production in PBMCs was not different among the three rhGM-CSFs at both 15 and 500 pM (Fig. 3B).

*3.4. Long-term biological activity of rhGM-CSF*

We then investigated the long-term biological effect of GM-CSF on TF-1 cells, monocytes, and PBMCs incubated for 72, 168, and 168 h, respectively. The effect on the proliferation/survival rate of TF-1 cells was significantly greater in cells incubated with 15 pM crhGM-CSF than that on cells incubated with the same concentration of erhGM-CSF or yrhGM-CSF. However, the effects were equivalent among the three rhGM-CSFs at 60 pM. The $ED_{50}$ of each rhGM-CSF was 21 and 24 pM for erhGM-CSF and yrhGM-CSF, respectively, whereas it was 3.9 pM for crhGM-CSF (Fig. 4A). When monocytes were incubated with the GM-CSFs, the proliferation/survival rate was higher at 4 pM crhGM-CSF than that of cells incubated with the same concentration of other GM-CSFs. The $ED_{50}$ was 10.7, 4.9, and 1.8 pM for erhGM-CSF, yrhGM-CSF, and crhGM-CSF, respectively (Fig. 4B). Similarly, the proliferation/survival rate of PBMCs was higher with 2–4 pM crhGM-CSF compared with that with other GM-CSFs (Fig. 4C). Proliferation/survival in the presence of goat anti-GM-CSF antibody was comparable, whereas the

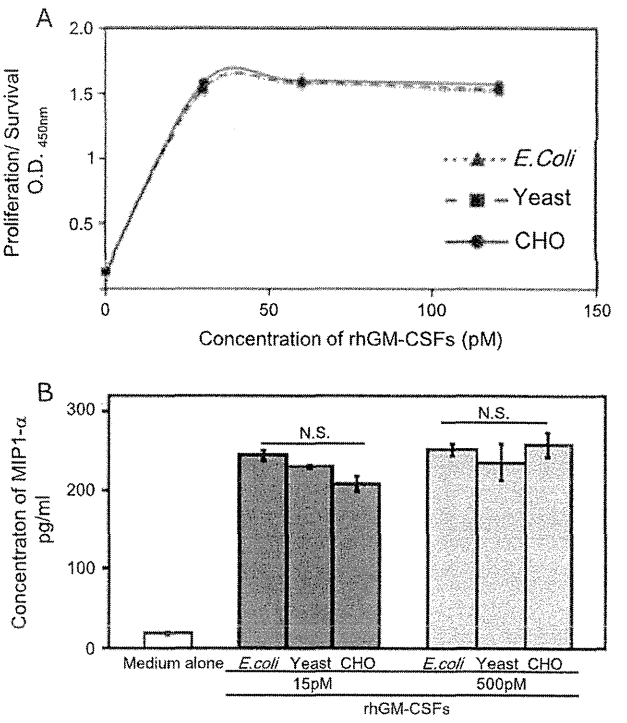


**Fig. 3.** Effect of intermediate-term stimulation (24 h) by rhGM-CSFs. (A) The proliferation/survival of TF-1 cells incubated for 24 h with various concentrations of rhGM-CSF derived from *E. coli* (N), yeast (j), and CHO (d) was measured by MTT assay, as described in Section 2. The vertical axis indicates formazan formation expressed as the OD at 450 nm. (B) MIP-1α production of PBMCs incubated for 24 h with 0, 15, or 500 pM of *E. coli*, yeast-, and CHO-derived rhGM-CSF was measured by ELISA as described in Section 2.

inhibitory effect of the antibody was highest in crhGM-CSF. These data suggested that the effect of crhGM-CSF on the proliferation/survival of TF-1 cells was not due to oligosaccharide moieties but rather due to the GM-CSF peptide (Fig. 4D). After 3-day incubation with 30 pM erhGM-CSF, yrhGM-CSF, or crhGM-CSF, the number of viable TF-1 cells increased by multiples of 1.95 ± 0.5, 2.0 ± 0.7, and 6.45 ± 0.25, respectively, compared with the number of viable cells before incubation (Fig. 4E). The size histogram of TF-1 cells incubated with crhGM-CSF displays a bimodal pattern with a mean value of 24.09 μm, which is larger than that of erhGM-CSF-treated cells (22.09 μm) and yrhGM-CSF-treated cells (22.0 μm) (Fig. 4F). The viability of crhGM-CSF-stimulated TF-1 cells was significantly higher than that of TF-1 cells stimulated with other rhGM-CSFs. These results demonstrate that low concentrations of crhGM-CSF not only promote proliferation/survival but also stimulate the growth of these cells more efficiently than do erhGM-CSF and yrhGM-CSF, and that the long-term effect of rhGM-CSF differs from the short- and intermediate-term outcomes. The long-term effects of erhGM-CSF and yrhGM-CSF for each condition were similar.

### 3.5. Modified bioactivity of crhGM-CSF after treatment with sialidase

To investigate the effect of sialyl residues located at the distal end of the oligosaccharide moieties [20] on cell proliferation/survival, we studied sialidase-treated crhGM-CSF. After treatment, mass spectrometry revealed a drastic reduction in the intensity of peaks corresponding to mono-, di-, tri-, and tetra-sialyl carbohydrates (Fig. 5A). This is also consistent with the banding pattern

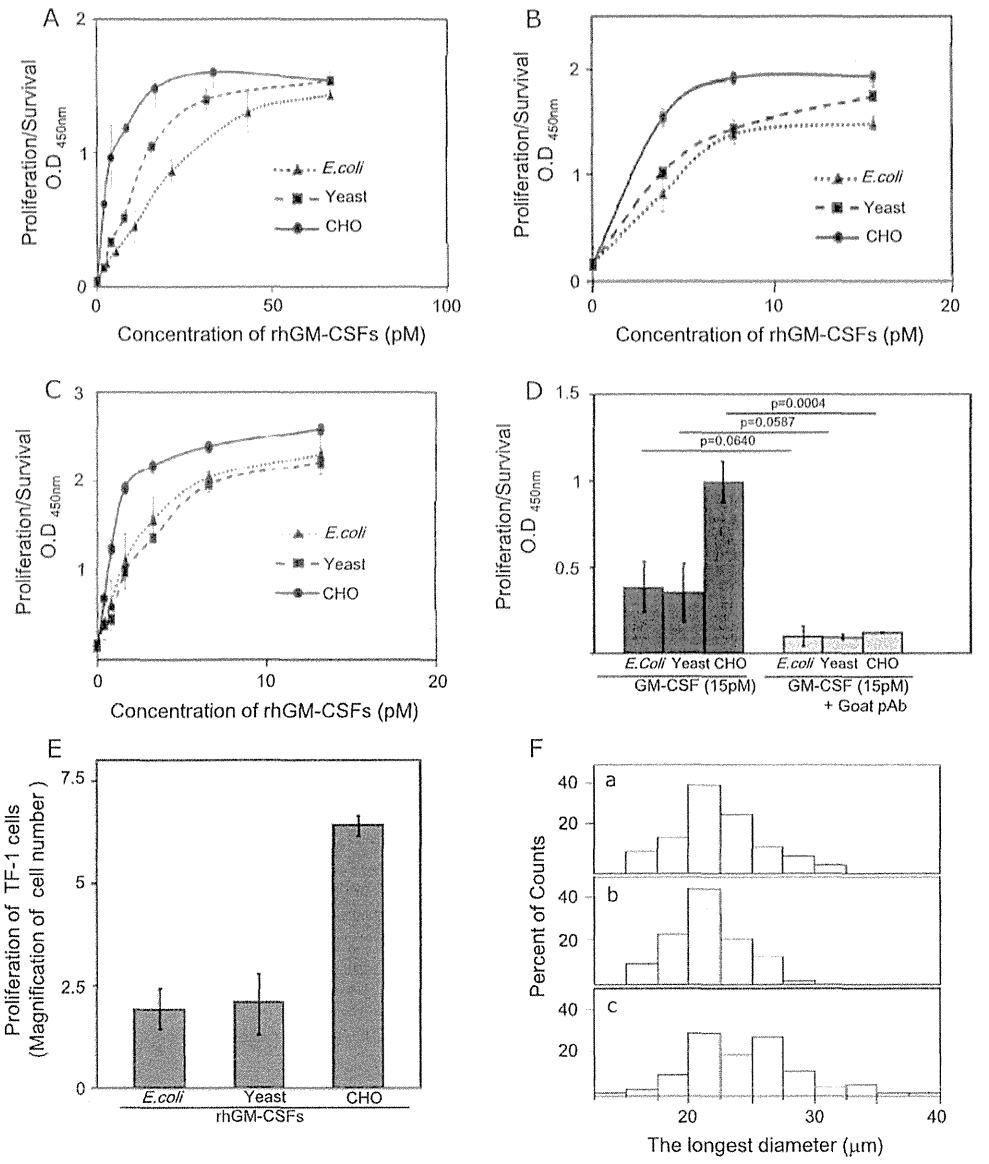


**Fig. 4.** Effect of long-term stimulation with various concentrations of rhGM-CSFs on the proliferation/survival of TF-1 cells, monocytes, and PBMCs. (A) Proliferation/survival of TF-1 cells incubated for 72 h with various concentrations (0–60 pM) of rhGM-CSF derived from *E. coli* (N), yeast (j), and CHO (d) was measured as described in Section 2. (B) Proliferation/survival of monocytes incubated for 168 h with various concentrations (0–15 pM) of rhGM-CSF derived from *E. coli* (N), yeast (j), and CHO (d) was measured as described in Section 2. (C) Proliferation/survival of PBMCs incubated for 168 h with various concentrations (0–15 pM) of rhGM-CSF derived from *E. coli* (N), yeast (j), and CHO (d) was measured as described in Section 2. (D) Effect of neutralizing goat anti-*E. coli*-derived GM-CSF antibody on the proliferation/survival of TF-1 cells incubated with 15 pM rhGM-CSFs. The vertical axis is the proliferation/survival of TF-1 cells (OD at 450 nm). (E) Magnification of proliferation was measured by enumerating viable TF-1 cells under a phase contrast microscopy before and after 72 h incubation with 30 pM rhGM-CSFs. (F) Size distribution of TF-1 cells incubated with 15 pM rhGM-CSFs for 72 h. The horizontal axis is the largest diameter of cells and the vertical axis is the number of cells.

obtained by SDS–PAGE, in which several bands characteristic for crhGM-CSF are absent or weaker (Fig. 5B). Desialylation of crhGM-CSF markedly reduced the proliferation/survival rates to levels observed with erhGM-CSF- or yrhGM-CSF-treated cells (Fig. 5C). These results suggest that the up-regulated proliferation/survival induced by crhGM-CSF is likely due to its sialyl residues.

### 3.6. The effect of GM-CSF on apoptosis of TF-1 cells

The effect of GM-CSF on the apoptosis of TF-1 cells was evaluated by Annexin V expression with flow cytometry. When TF-1 cells were incubated with 30 pM crhGM-CSF for 3 days, 8.8% of the cells were apoptotic. In contrast, 17.0%, 21.4%, and 15.9% of cells were apoptotic upon incubation with erhGM-CSF, yrhGM-CSF, and sialidase-treated crhGM-CSF, respectively (Fig. 6A). TF-1 cells incubated with crhGM-CSF had fewer vacuolated nuclei and coagulated chromatin than those of cells incubated with other GM-CSFs (Fig. 6B). TF-1 cell apoptosis was also confirmed by DNA ladder formation via agarose gel electrophoresis (Fig. 6C). These results suggested that apoptotic TF-1 cells were less frequently observed in the presence of low concentration of crhGM-CSF than erhGM-CSF, yrhGM-CSF and sialidase-treated crh GM-CSF as TF-1 cells are GM-CSF dependent cell line. It is plausible that GM-CSF bioactivity is likely to remain in culture supernatant of the cells incubated with crhGM-CSF compared with other rhGM-CSFs.

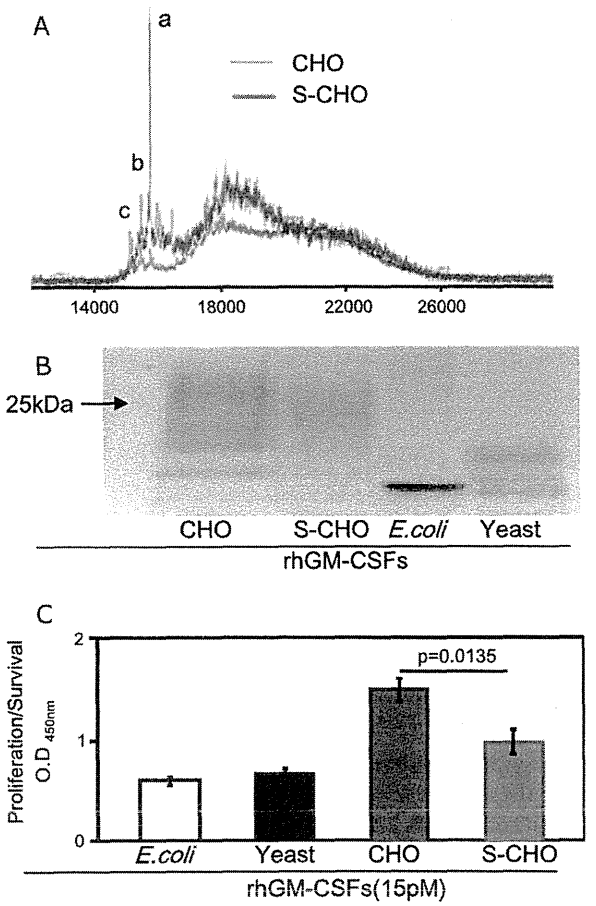


**Fig. 5.** Sialidase treatment of CHO-cell-derived rhGM-CSF and its biological activity. (A) Mass spectra of CHO cell-derived rhGM-CSF before (blue line) and after (red line) treatment with sialidase. (B) SDS–PAGE appearance of CHO cell-derived GM-CSF, CHO cell-derived GM-CSF after sialidase treatment, *E. coli*-derived GM-CSF, and yeast-derived GM-CSF. (C) The effect of sialidase treatment on the proliferation/survival of TF-1 cells after 72 h incubation with *E. coli*-, yeast-, CHO cells-derived rhGM-CSF or CHO cells-derived rhGM-CSF after sialidase treatment.

### 3.7. Clearance of rhGM-CSF by TF-1 cells and PBMCs

The clearance of crhGM-CSF by TF-1 cells and PBMCs was delayed compared with that of other GM-CSFs. After 24 and 48 h clearance assays, 13% and 9.5% of the initial crhGM-CSF concentration remained in the culture supernatant of PBMCs, whereas only 4.5% and 1.1% of erhGM-CSF, and 3.1%, 1% of yrhGM-CSF and 5.6% and 2.7% of sialidase-treated crhGM-CSF remained, respectively (Fig. 7A). On the other hand, after 24 and 48 h clearance assays, 7.5% and 3% of the initial crhGM-CSF concentration remained in the culture supernatant of TF-1 cells, whereas only 1.3% and 1.1% of erhGM-CSF, 1.1% and 1.0% of yrhGM-CSF and 2.9% and 2.7% of sialidase-treated crhGM-CSF remained, respectively (Fig. 7B). After 48 h incubation with erhGM-CSF, yrhGM-CSF, and sialidase treated crhGM-CSF, 15 pM of the same rhGM-CSF was except for crhGM-CSF added into each well. As shown in Fig. 7C, addition of each rhGM-CSF improved the proliferation/survival of TF-1 cells in the next 24 h reaching a similar level of those incubated with original 15 pM of crhGM-CSF for three days. Taken together with the data of proliferation/survival assay, it is likely that delayed clearance crhGM-CSF might prolong its biological activity *in vitro* (Fig. 7C).

## 4. Discussion

A number of studies have reported the expression of human GM-CSF by using natural or recombinant cells. These studies revealed that mammalian cells secrete GM-CSF proteins with variable molecular masses [20]. It has also been shown that its properties such as pharmacokinetics, binding affinity to the GM-CSF receptor, bioactivity, and immunogenicity are affected by glycosylation. In the present study, we demonstrated that compared with erhGM-CSF or yrhGM-CSF, crhGM-CSF promoted more efficiently the proliferation/survival of TF-1 cells, especially at low concentrations. In contrast to the results of the present study, natural hGM-CSF is thought to have lower biological activity with increasing glycosylation [15,24]. The pattern of glycosylation on GM-CSF has been found to affect its specific biological activity. Non-human expression systems such as yeast-, CHO cell-, or COS cell-derived rhGM-CSFs have distinct carbohydrate moieties and show different biological activities [18,28]. The half-life of hGM-CSF injected into rats decreases upon deglycosylation, indicating that the carbohydrate moieties influence the clearance, increase the stability, or alter the distribution of hGM-CSF. The carbohydrate structure of hematopoietic growth factors may therefore be important in determining their effective half-life *in vivo*. In this regard, we confirmed that *in vitro* GM-CSF clearance was also affected largely by the carbohydrate moieties of GM-CSF, especially its sialyl residues at the distal end of the oligosaccharide moieties.

The significance of the glycosylation of hematopoietic growth factors has been investigated previously. First, it is important for the secretion of glycoproteins. Erythropoietin secretion is prevented by site-directed mutagenesis of the N- or O-linked glycosylation sites [29–31]. As tunicamycin does not interfere with secretion of hGM-CSF, the N-linked carbohydrate is not crucial for this process [32]. Second, the N-linked carbohydrate influences the biological activity and receptor binding of other glycoprotein hormones and cytokines [29,33]. The *in vitro* activity of erythropoietin requires oligosaccharide moieties, but N-linked carbohydrates markedly reduce the *in vitro* activity of calcitonin. Glycosylation of luteinizing hormone is required for signal transduction, although

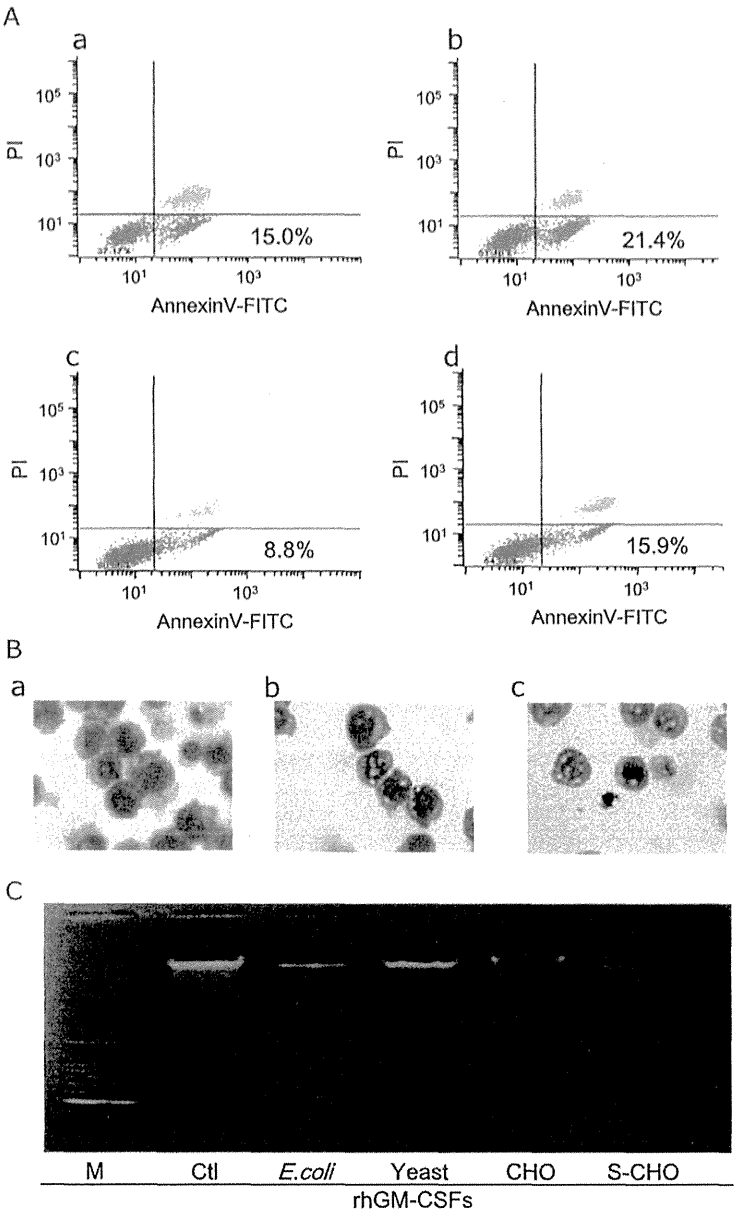


**Fig. 6.** Apoptosis of TF-1 cells incubated with 30 pM rhGM-CSFs for 72 h. (A) Flow cytometry results for apoptotic TF-1 cells incubated with rhGM-CSF derived from *E. coli* (a), yeast (b), CHO cells (c), or sialidase-treated CHO cells (d). The horizontal axis is the fluorescence intensity of Annexin V-FITC and the vertical axis is the fluorescence intensity of propidium iodide. (B) Morphology of TF-1 cells incubated with GM-CSF derived from CHO cells (a), yeast (b), and *E. coli* (c) at high magnification (1000×). Cells were cytocentrifuged and stained with Diff-Quick stain. (C) Agarose gel electropherogram of DNA extracted from TF-1 cells incubated with *E. coli*-, yeast-, CHO cells-derived rhGM-CSF or CHO cells-derived rhGM-CSF after sialidase treatment.

deglycosylated luteinizing hormone has higher receptor binding affinity [33]. Similarly, deglycosylation of hGM-CSF increases the receptor binding affinity [15]. However, in contrast to hGM-CSF, the most active forms are heavily glycosylated in luteinizing hormone [32].

Sialyl residues on carbohydrates in crhGM-CSF are considered crucial to the upregulation of the proliferation/survival of TF-1 cells because desialylation remarkably reduces this effect. Various sialylated forms of GM-CSF are produced in various tissues of mice and confer different physicochemical characteristics to murine GM-CSF [34]. Molecular weights of GM-CSF purified from various organs range from 37 to 200 kDa [32]; thus, it is possible that the bioactivity of GM-CSF produced in different tissues is regulated by the degree of sialylation. Since sialyl residues at the distal end of oligosaccharides can affect the specific activity of hGM-CSF as well as its isoelectric points and affinities to the GM-CSF receptor, sialylation may alter the activity of hGM-CSF in a tissue-specific manner. The aforementioned studies are clinically important because therapy using hGM-CSF has been associated with side effects, which may relate to its activities as a mediator of inflammation rather than to its function as a growth factor [15]. If different glycosylation patterns allow hGM-CSF activity to be regulated, manipulation of the carbohydrate moieties may enable reduction of the inflammatory mediator effects of hGM-CSF without affecting the stimulation of myeloid cell production.

GM-CSF exerts its biological activities by binding to specific high-affinity cell-surface receptors. After binding, the ligand/receptor complex is rapidly internalized in most hematopoietic cells [35,36]. It is not fully known whether the turnover time of this internalization differs between different rhGM-CSFs. It is possible

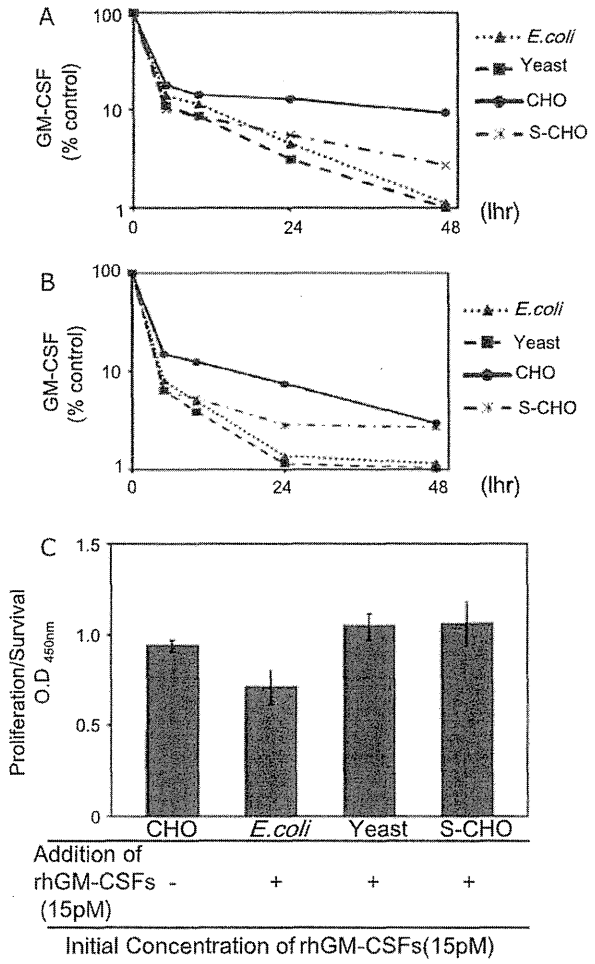


**Fig. 7.** GM-CSF clearance assay of TF-1 cells and peripheral blood mononuclear cells. (A) Peripheral blood mononuclear cells were incubated for 0–48 h with each 15 pM of *E. coli*-, yeast-, CHO cells-derived rhGM-CSF or CHO cells-derived rhGM-CSF after sialidase treatment. (B) TF-1 cells were incubated for 0–48 h with each 15 pM of *E. coli*-, yeast-, CHO cells-derived rhGM-CSF or CHO cells-derived rhGM-CSF after sialidase treatment. The horizontal axis is the time after the start of incubation. The vertical access is percent each rhGM-CSF concentration per initial concentration at each time point in the culture supernatant. (C) After 48 h incubation with *E. coli*-, yeast-, CHO cells-derived rhGM-CSF or CHO cells-derived rhGM-CSF after sialidase treatment, 15 pM of the same rhGM-CSF was added into each well. The vertical axis is the proliferation/survival of TF-1 cells (OD at 450 nm).

that the oligosaccharide sialyl residue of crhGM-CSF can attenuate its binding to the low-affinity rhGM-CSF receptor α and/or associate with the rhGM-CSF β chain, resulting in downregulation of signal transduction and delayed clearance of the molecule [15]. The present study revealed that stimulation with low concentrations of crhGM-CSF augmented STAT5 phosphorylation less effectively than did low concentrations of erhGM-CSF and yrhGM-CSF. The sialyl residue may prolong the turnover cycle (known to be 40 s for erhGM-CSF) and thus maintain rhGM-CSF bioactivity for a longer period [35]. In the future, it is necessary to determine whether the sialyl residues of GM-CSF attenuate its binding to low-affinity receptors on hematopoietic cells or delay the process of its internalization into cells.

## 5. Conclusion

We have demonstrated for the first time that sialylated oligosaccharide moieties prolong the proliferation/survival of rhGM-CSF *in vitro*. Further studies are warranted to determine the correlation of the oligosaccharide structure of crhGM-CSF with both signal transduction and internalization.

## Authorship

A. Hashimoto and K. Nakata wrote the manuscript and designed the project.

A. Hashimoto performed experiments. Y. Ito and A. Yamagata assisted technical issues. T. Tanaka and N. Kitamurta contributed to the statistical analysis of data. R. Tazawa participated in preparation of materials. K. Nakagaki provided variable information for methods. All authors read and approved the final manuscript.

## Disclosure

The authors declare that they have no competing interests.

## Acknowledgments

The authors thank JCR Pharmaceuticals Co., Ltd. for providing valuable information on recombinant Chinese hamster ovary cell derived GM-CSF. We also thank Takuji Suzuki, Kiyoko Akagawa, Tomoyuki Kawase, Takahito Nei, Takuro Sakagami and Kanji Uchida for valuable discussions and critical review of this manuscript. We appreciate Maiko Higuchi for technical help and Marie Mori for assistance of manuscript submission.

## References

[1] Atkinson YH, Lopez AF, Marasco WA, Lucas CM, Wong GG, Burns GF, et al. Recombinant human granulocyte–macrophage colony-stimulating factor (rH GM-CSF) regulates f Met-Leu-Phe receptors on human neutrophils. Immunology 1988;64:519–25.
[2] Burgess AW, Begley CG, Johnson GR, Lopez AF, Williamson DJ, Mermod JJ, et al. Purification and properties of bacterially synthesized human granulocyte–macrophage colony stimulating factor. Blood 1987;69:43–51.
[3] Metcalf D. Hematopoietic cytokines. Blood 2008;111:485–91.
[4] Esnault S, Malter JS. GM-CSF regulation in eosinophils. Arch Immunol Ther Exp (Warsz) 2002;50:121–30.
[5] Guthridge MA, Stomski FC, Thomas D, Woodcock JM, Bagley CJ, Berndt MC, et al. Mechanism of activation of the GM-CSF, IL-3, and IL-5 family of receptors. Stem Cells 1998;16:301–13.
[6] Hansen G, Hercus TR, McClure BJ, Stomski FC, Dottore M, Powell J, et al. The structure of the GM-CSF receptor complex reveals a distinct mode of cytokine receptor activation. Cell 2008;134:496–507.
[7] Martinez-Moczygemba M, Huston DP. Biology of common beta receptor-signaling cytokines: IL-3, IL-5, and GM-CSF. J Allergy Clin Immunol 2003;112:653–65 [quiz 66].
[8] Tanaka T, Motoi N, Tsuchihashi Y, Tazawa R, Kaneko C, Nei T, et al. Adult-onset hereditary pulmonary alveolar proteinosis caused by a single-base deletion in CSF2RB. J Med Genet 2011;48:205–9.
[9] Hercus TR, Thomas D, Guthridge MA, Ekert PG, King-Scott J, Parker MW, et al. The granulocyte–macrophage colony-stimulating factor receptor: linking its structure to cell signaling and its role in disease. Blood 2009;114:1289–98.
[10] Trapnell BC, Whitsett JA. Gm-CSF regulates pulmonary surfactant homeostasis and alveolar macrophage-mediated innate host defense. Annu Rev Physiol 2002;64:775–802.
[11] Huang FF, Barnes PF, Feng Y, Donis R, Chroneos ZC, Idell S, et al. GM-CSF in the lung protects against lethal influenza infection. Am J Respir Crit Care Med 2011;184:259–68.
[12] Weisbart RH, Golde DW, Clark SC, Wong GG, Gasson JC. Human granulocyte–macrophage colony-stimulating factor is a neutrophil activator. Nature 1985;314:361–3.
[13] Socinski MA, Cannistra SA, Sullivan R, Elias A, Antman K, Schnipper L, et al. Granulocyte–macrophage colony-stimulating factor induces the expression of the CD11b surface adhesion molecule on human granulocytes *in vivo*. Blood 1988;72:691–7.
[14] Shibata Y, Berclaz PY, Chroneos ZC, Yoshida M, Whitsett JA, Trapnell BC. GM-CSF regulates alveolar macrophage differentiation and innate immunity in the lung through PU.1. Immunity 2001;15:557–67.
[15] Cebon J, Nicola N, Ward M, Gardner I, Dempsey P, Layton J, et al. Granulocyte–macrophage colony stimulating factor from human lymphocytes. The effect of glycosylation on receptor binding and biological activity. J Biol Chem 1990;265:4483–91.
[16] Broudy VC, Kaushansky K, Segal GM, Harlan JM, Adamson JW. Tumor necrosis factor type alpha stimulates human endothelial cells to produce granulocyte/

macrophage colony-stimulating factor. Proc Natl Acad Sci USA 1986;83:7467–71.
[17] Fibbe WE, van Damme J, Billiau A, Voogt PJ, Duinkerken N, Kluck PM, et al. Interleukin-1 (22-K factor) induces release of granulocyte–macrophage colony-stimulating activity from human mononuclear phagocytes. Blood 1986;68:1316–21.
[18] Lee F, Yokota T, Otsuka T, Gemmell L, Larson N, Luh J, et al. Isolation of cDNA for a human granulocyte–macrophage colony-stimulating factor by functional expression in mammalian cells. Proc Natl Acad Sci USA 1985;82:4360–4.
[19] Gabrilove JL, Welte K, Harris P, Platzer E, Lu L, Levi E, et al. Pluripoietin alpha: a second human hematopoietic colony-stimulating factor produced by the human bladder carcinoma cell line 5637. Proc Natl Acad Sci USA 1986;83:2478–82.
[20] Forno G, Bollati Fogolin M, Oggero M, Kratje R, Etcheverrigaray M, Conradt HS, et al. N- and O-linked carbohydrates and glycosylation site occupancy in recombinant human granulocyte–macrophage colony-stimulating factor secreted by a Chinese hamster ovary cell line. Eur J Biochem 2004;271:907–19.
[21] Sieff CA. Hematopoietic growth factors. J Clin Invest 1987;79:1549–57.
[22] Kitamura T, Tange T, Terasawa T, Chiba S, Kuwaki T, Miyagawa K, et al. Establishment and characterization of a unique human cell line that proliferates dependently on GM-CSF, IL-3, or erythropoietin. J Cell Physiol 1989;140:323–34.
[23] Dorr RT. Clinical properties of yeast-derived versus *Escherichia coli*-derived granulocyte–macrophage colony-stimulating factor. Clin Ther 1993;15:19–29 [discussion 18].
[24] Moonen P, Mermod JJ, Ernst JF, Hirschi M, DeLamarter JF. Increased biological activity of deglycosylated recombinant human granulocyte/macrophage colony-stimulating factor produced by yeast or animal cells. Proc Natl Acad Sci USA 1987;84:4428–31.
[25] Uchida K, Nakata K, Suzuki T, Luisetti M, Watanabe M, Koch DE, et al. Granulocyte/macrophage-colony-stimulating factor autoantibodies and myeloid cell immune functions in healthy subjects. Blood 2009;113:2547–56.
[26] Rosen LB, Freeman AF, Yang LM, Jutivorakool K, Olivier KN, Angkasekwinai N, et al. Anti-GM-CSF autoantibodies in patients with cryptococcal meningitis. J Immunol 2013;190:3959–66.
[27] Uchida K, Beck DC, Yamamoto T, Berclaz PY, Abe S, Staudt MK, et al. GM-CSF autoantibodies and neutrophil dysfunction in pulmonary alveolar proteinosis. N Engl J Med 2007;356:567–79.
[28] Nicola NA, Metcalf D, Johnson GR, Burgess AW. Separation of functionally distinct human granulocyte–macrophage colony-stimulating factors. Blood 1979;54:614–27.
[29] Dube S, Fisher JW, Powell JS. Glycosylation at specific sites of erythropoietin is essential for biosynthesis, secretion, and biological function. J Biol Chem 1988;263:17516–21.
[30] Teh SH, Fong MY, Mohamed Z. Expression and analysis of the glycosylation properties of recombinant human erythropoietin expressed in *Pichia pastoris*. Genet Mol Biol 2011;34:464–70.
[31] Darling RJ, Kuchibhotla U, Glaesner W, Micanovic R, Witcher DR, Beals JM. Glycosylation of erythropoietin affects receptor binding kinetics: role of electrostatic interactions. Biochemistry 2002;41:14524–31.
[32] Jonathan Cebon, Burgess Antony W. Glycosylation of human granulocyte-macrophage colony stimulating factor alters receptor binding and biological activity. TIGG 1991;3(12).
[33] Sairam MR, Bhargavi GN. A role for glycosylation of the alpha subunit in transduction of biological signal in glycoprotein hormones. Science 1985;229:65–7.
[34] Walker F, Burgess AW. Specific binding of radioiodinated granulocyte-macrophage colony-stimulating factor to hemopoietic cells. Embo J 1985;4:933–9.
[35] Elliott MJ, Moss J, Dottore M, Park LS, Vadas MA, Lopez AF. Differential binding of IL-3 and GM-CSF to human monocytes. Growth Factors 1992;6:15–29.
[36] Walker F, Burgess AW. Internalisation and recycling of the granulocyte-macrophage colony-stimulating factor (GM-CSF) receptor on a murine myelomonocytic leukemia. J Cell Physiol 1987;130:255–61.

CHEST

Original Research

DIFFUSE LUNG DISEASE

# Duration of Benefit in Patients With Autoimmune Pulmonary Alveolar Proteinosis After Inhaled Granulocyte-Macrophage Colony-Stimulating Factor Therapy

*Ryushi Tazawa, MD; Yoshikazu Inoue, MD; Toru Arai, MD; Toshinori Takada, MD; Yasunori Kasahara, MD, FCCP; Masayuki Hojo, MD; Shinya Ohkouchi, MD; Yoshiko Tsuchihashi, MD; Masanori Yokoba, MD; Ryosuke Eda, MD; Hideaki Nakayama, MD; Haruyuki Ishii, MD; Takahito Nei, MD; Konosuke Morimoto, MD; Yasuyuki Nasuhara, MD, FCCP; Masahito Ebina, MD; Masanori Akira, MD; Toshio Ichiwata, MD; Koichiro Tatsumi, MD, FCCP; Etsuro Yamaguchi, MD; and Koh Nakata, MD*

***Background:*** **Treatment of autoimmune pulmonary alveolar proteinosis (aPAP) by subcutaneous injection or inhaled therapy of granulocyte-macrophage colony-stimulating factor (GM-CSF) has been demonstrated to be safe and efficacious in several reports. However, some reports of subcutaneous injection described transient benefit in most instances. The durability of response to inhaled GM-CSF therapy is not well characterized.**

***Methods:*** **To elucidate the risk factors for recurrence of aPAP after GM-CSF inhalation, 35 patients were followed up, monitoring for the use of any additional PAP therapies and disease severity score every 6 months. Physiologic, serologic, and radiologic features of the patients were analyzed for the findings of 30-month observation after the end of inhalation therapy.**

***Results:*** **During the observation, 23 patients remained free from additional treatments, and twelve patients required additional treatments. There were no significant differences in age, sex, symptoms, oxygenation indexes, or anti-GM-CSF antibody levels at the beginning of treatment between the two groups. Baseline vital capacity (% predicted, %VC) were higher among those who required additional treatment ($P < .01$). Those patients not requiring additional treatment maintained the improved disease severity score initially achieved. A significant difference in the time to additional treatment between the high %VC group (%VC ≥ 80.5) and the low %VC group was seen by a Kaplan-Meier analysis and a log-rank test ($P < .0005$).**

***Conclusions:*** **These results demonstrate that inhaled GM-CSF therapy sustained remission of aPAP in more than one-half of cases, and baseline %VC might be a prognostic factor for disease recurrence.**

***Trial registry:*** **ISRCTN Register and JMACCT Clinical Trial Registry; No.: ISRCTN18931678 and JMAIIA00013; URL: http://www.isrctn.org and http://www.jmacct.med.or.jp**

***CHEST 2014; 145(4):729–737***

**Abbreviations:** A-a$DO_2$ = alveolar-arterial oxygen difference; Ab = antibody; aPAP = autoimmune pulmonary alveolar proteinosis; AT = additional treatment; BALF = BAL fluid; CEA = carcinoembryonic antigen; DLCO = diffusing capacity of the lung for carbon monoxide; DSS = disease severity score; FR = free from additional treatment; GM-CSF = granulocyte-macrophage colony-stimulating factor; IQR = interquartile range; KL-6 = Krebs von den Lungen-6; LDH = lactate dehydrogenase; PAP = pulmonary alveolar proteinosis; ROC = receiver operating characteristics curve; SP = surfactant protein; VC = vital capacity; WLL = whole-lung lavage

Autoimmune pulmonary alveolar proteinosis (aPAP) is a rare lung disease characterized by the accumulation of surfactant protein (SP), which causes progressive respiratory insufficiency.[1-3] The pathogenesis has been attributed to the excessive production of a neutralizing autoantibody against granulocyte-macrophage colony-stimulating factor (GM-CSF) that impairs GM-CSF-dependent surfactant clearance mediated by

alveolar macrophages.[4-8] On pulmonary function testing, the most common pattern seen is that of a restrictive defect, with a disproportionate reduction in diffusing capacity of the lung for carbon monoxide (DLCO) relative to a modest impairment of vital capacity (VC).[2] The disease is usually treated by whole-lung lavage (WLL), which remains the standard therapy to date.

The first patient successfully treated with subcutaneously administered GM-CSF was reported in 1996.[9] In an international multicenter phase 2 trial study, 14 patients were treated with GM-CSF by subcutaneous injection in escalating doses over a 3-month period, with an overall response rate of 43%.[10,11] A subsequent single-center study of 21 patients with aPAP treated with GM-CSF by subcutaneous administration in escalating doses for 6 to 12 months reported an overall response rate of 48%.[12] Several single cases of subcutaneous GM-CSF therapy have reported similar outcomes.[13,14] However, local reaction at sites of injection and other minor toxicities occurred in 85% of patients receiving subcutaneous GM-CSF.[2]

Manuscript received March 12, 2013; revision accepted October 1, 2013.

**Affiliations:** From the Niigata University Medical and Dental Hospital (Drs Tazawa and Nakata), Niigata; the National Hospital Organization (NHO) Kinki-Chuo Chest Medical Center (Drs Inoue, Arai, and Akira), Osaka; the Niigata University Graduate School of Medical and Dental Sciences (Drs Takada and Nakayama), Niigata; the Department of Respirology (Drs Kasahara and Tatsumi), Graduate School of Medicine, Chiba University, Chiba; the Division of Respiratory Medicine (Dr Hojo), National Center for Global Health and Medicine, Tokyo; the Department of Respiratory Medicine (Drs Ohkouchi and Ebina), Tohoku University Medical School, Sendai; the Juzenkai Hospital (Dr Tsuchihashi), Nagasaki; the Institute of Tropical Medicine (Drs Tsuchihashi and Morimoto), Nagasaki University, Nagasaki; the Kitasato University School of Allied Health Sciences (Dr Yokoba), Kanagawa; the NHO Yamaguchi-Ube Medical Center (Dr Eda), Ube; the Kurashiki Municipal Kojima Hospital (Dr Eda), Kurashiki; the Department of Respiratory Medicine (Dr Nakayama), Tokyo Medical University, Tokyo; the Department of Respiratory Medicine (Dr Ishii), Kyorin University School of Medicine, Tokyo; the Department of Respiratory Medicine (Dr Nei), Nippon Medical University School of Medicine, Tokyo; the First Department of Medicine (Dr Nasuhara), Hokkaido University School of Medicine, Sapporo; the Department of Respiratory Medicine (Dr Ichiwata), Tokyo Medical University Hachioji Medical Center, Tokyo; and the Division of Respiratory Medicine and Allergology (Dr Yamaguchi), Department of Medicine, Aichi Medical University School of Medicine, Aichi, Japan.

**Funding/Support:** This work was supported in part by grants from the Japanese Ministry of Education and Science, Ministry of Health, Labour, and Welfare of Japan [Grant H14-trans-014 to Dr Nakata, H21-Nanchi-Ippan-161 to Dr Inoue, and H24-Rinkensui-Ippan-003 to Dr Tazawa], Grant-in-Aid for Scientific Research [Category B 18406031 to Dr Inoue and Category C 22590852 to Dr Tazawa], and National Hospital Organization of Japan [Category Network to Dr Inoue].

**Correspondence to:** Koh Nakata, MD, Niigata University Medical & Dental Hospital, Bioscience Medical Research Center, 1-754 Asahimachi-dori, Chuo-ku Niigata, Niigata, Japan 951-8520; e-mail: radical@med.niigata-u.ac.jp



**DOI: 10.1378/chest.13-0603**

GM-CSF inhalation is a promising alternative therapy for aPAP that has been demonstrated to lead to functional, biologic, and radiologic improvement.[15-18] Our national, multicenter phase 2 study revealed that the therapy reduced alveolar-arterial oxygen difference (A-a$DO_2$) by 12.3 mm Hg in 35 patients who completed the therapy, resulting in 24 responders. No treatment-related side effects were noted. Of importance, our previous phase 2 study showed that there was no significant difference in serologic, physiologic, and CT scan testing, except for serum Krebs von den Lungen-6 (KL-6) levels, between the responders and the nonresponders.[18]

There is limited information regarding the duration of benefit after various treatments of aPAP. In the literature analysis of 55 cases with a therapeutic response to WLL, the median duration of clinical benefit from lavage was 15 months.[2] A phase 2 study of subcutaneous GM-CSF administration demonstrated that 45% of patients required WLL during follow-up observation of 39 ± 17.3 months.[12] In a retrospective analysis of inhaled GM-CSF therapy (250 μg bid), five of 12 patients manifest progressive disease during observation.[17] As the disease progresses very slowly and can fluctuate in some cases, it is necessary to evaluate the prognosis by monitoring prospectively at the same time points after the treatment and by disease severity score as well as the need for additional treatment. The aim of this study was to define the duration of benefit among patients who underwent GM-CSF inhalation therapy.

## Materials and Methods

### *Patients and Protocols*

The present study prospectively observed patients who participated in a multicenter phase 2 trial (35 patients, registered as ISRCTN18931678 and JMAIIA00013) of GM-CSF inhalation therapy described previously. In brief, patients who had lung biopsy or cytologic findings diagnostic for pulmonary alveolar proteinosis (PAP), including elevated serum anti-GM-CSF antibody (Ab) levels and no improvement during a 12-week observation period, entered the treatment phase. Recombinant human GM-CSF dissolved in 2 mL of sterile saline was inhaled using an LC-PLUS nebulizer (PARI International). The treatment consisted of high-dose GM-CSF administration (125 μg bid on days 1-8, none on days 9-14; sargramostim) for six repetitions of 2-week cycles, then low-dose administration (125 μg once daily on days 1-4, none on days 5-14) for six repetitions of 2-week cycles (for a total dose of 15 mg). The clinical information including physiologic, serologic, and radiologic features obtained[18] was compared with the results of the following 30-month observation.

Patients were regularly evaluated by their physicians at the network hospitals after the GM-CSF inhalation therapy. The worsening dyspnea was evaluated with pulse oximetry, arterial blood gas analysis, or both in outpatient settings. Disease severity in patients was evaluated using PAP disease severity score (DSS) described previously.[19] Patients underwent additional treatments based on

either of the following criteria: (1) DSS is 3 or 4 and symptoms are worsening or (2) DSS 5, as shown in Figure 1. The consortium office of Niigata University contacted the network hospitals every 6 months with a questionnaire regarding additional treatment and disease severity score of the patient. The follow-up clinical information obtained at each network hospital was entered into a database to be compared with the results of the baseline clinical evaluation of each patient. The data were collected from nine clinical research centers in Japan (Hokkaido University, Tohoku University, Chiba University, Kitasato University, Niigata University, Aichi Medical University, National Hospital Organization Kinki-Chuo Chest Medical Center, National Hospital Organization Yamaguchi-Ube Medical Center, and Nagasaki University Institute of Tropical Medicine).

The study was approved by institutional review board of Niigata University (approval No. NH17-006) and the institutional review boards at all participating centers. Informed consent was obtained from all control subjects. The clinical information obtained by the clinical studies was entered into a database to be compared with the results of the 30-month observation. The study was designed and monitored for data quality and safety by a steering committee composed of the principal investigator at each participating site. The steering committee held a conference twice a year, where the findings of the observation were monitored.

*BAL Procedures and GM-CSF Autoantibodies*

The steering committee edited a standard operational procedure for BAL, which was followed by all participating institutes and described previously.[18,20] The concentration of GM-CSF autoantibodies in BAL fluid (BALF) or in serum were measured using a sandwich enzyme-linked immunosorbent assay as described previously.[4,21]

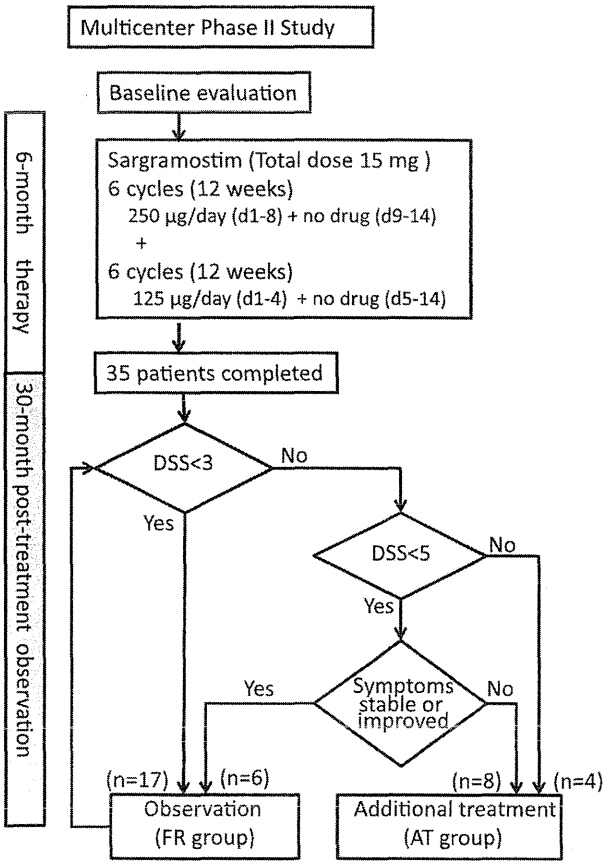


FIGURE 1. Profile of the study cohort. AT = additional treatment; DSS = disease severity score; FR = free from additional treatment.

*Statistical Analysis*

Numerical results are presented as the mean ± SE or the median and interquartile range (IQR). The $\chi^2$ test was used to evaluate proportions for variables between high and low responders. The paired *t* test was used for comparisons between normally distributed data and the treatment periods. Comparisons of nonparametric data were made using the Wilcoxon signed-rank test. For group comparisons, unpaired *t* tests and Wilcoxon rank-sum tests were used. All *P* values were reported as two-sided. Analysis was performed using JMP software, version 8.0.2 (SAS Institute Inc).

## RESULTS

### *Patient Characteristics and Requirements for Additional Treatments as an Indicator of Recurrence*

Demographic data of patients are shown in Table 1. During the 30 months of observation after the end of GM-CSF inhalation, the need for treatments was monitored as an indicator of disease recurrence in each patient. Twenty-three patients were free from additional treatments during 30 months of observation and were designated as FR (free from additional treatment). Twelve patients who required additional treatments, including six patients with recurrence described in our previous study,[18] were designated as AT (additional treatment). Of those, two patients maintained most severe disease (DSS 5) even after the GM-CSF treatment and underwent subsequent WLL. One patient who had dyspnea, cough, and sputum production did not respond to the GM-CSF treatment and underwent subsequent WLL. One patient with cough and dyspnea showed worsening in $PaO_2$ and cough and had WLL 12 months after the GM-CSF inhalation. The other eight patients with dyspnea showed worsening in $PaO_2$/oxygen saturation by pulse oximetry (two patients worsened to DSS 5) and underwent additional therapy (e-Fig 1); five underwent additional GM-CSF inhalation treatments, two had WLL, and one patient, a nonresponder, declined WLL and underwent acetylcysteine inhalation, showing much improvement in hypoxia. Median time to additional treatment of the 12 patients was 50.5 weeks, with a range of 8.5 to 117.5 weeks. There was no significant difference in age, sex, symptoms, smoking status, history of dust exposure, arterial blood gas analysis, numbers of responders to GM-CSF inhalation, history of previous lung lavage, and anti-GM-CSF-Ab titer between the FR and AT groups (Table 1). There was no significant difference in disease markers, including baseline levels of $PaO_2$, $A\text{-}aDO_2$, %VC, %DLCO, CT scan scores, lactate dehydrogenase (LDH), and KL-6 between the patients who underwent WLL (n = 6, AT-WLL group) and those treated with GM-CSF inhalation (n = 5, AT-GM group)